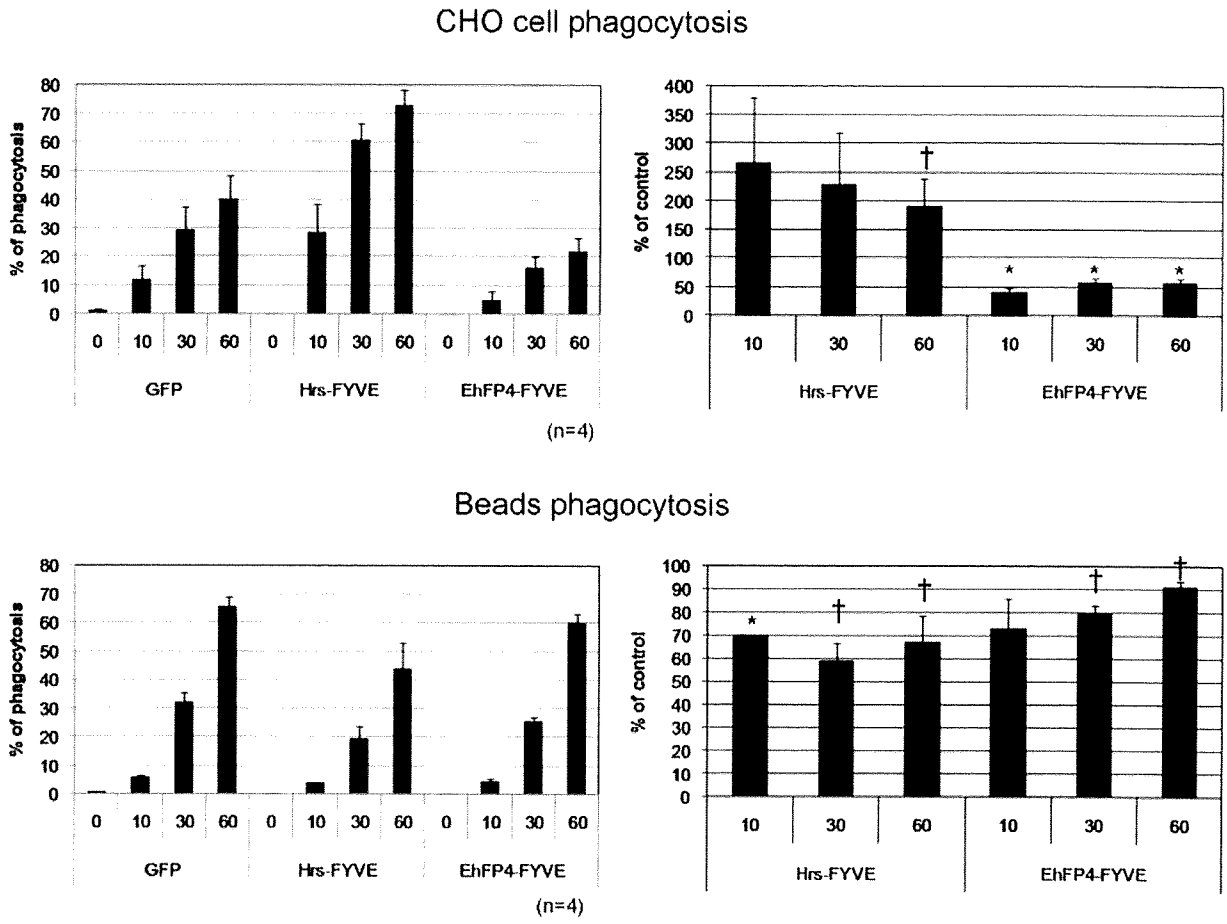

Fig. 6. Effects of Hrs–FYVE and EhFP4-FYVE overexpression on phagocytosis of CHO cells and carboxylated beads. GFP–Hrs–FYVE, GFP–EhFP4–FYVE and GFP transformants were mixed with either CHO cells (top panels) or carboxylated beads (bottom panels) for 0, 10, 30 and 60 min, and the percentage of cells that ingested cells or beads at each time point was calculated (left panels). The percentage of cells that ingested CHO cells or beads in GFP–Hrs–FYVE and GFP–EhFP4–FYVE transformants was also normalized against that of the control GFP transformant and shown in percentage (right panels). The mean and standard deviation of four independent experiments are shown. Asterisks or crosses indicate statistical significance at $P < 0.01$ or $P < 0.05$ respectively, by Student's *t*-test.

et al., 2001; Yu *et al.*, 2008). Interestingly, in *C. elegans*, Rab7, but not PtdIns(3)P, was shown to localize to the structure. These data suggest that interorganelle trafficking via the thread-like structure may be conserved among various organisms, but its components may vary.

Unique expansion of the FYVE-domain-containing protein family in E. histolytica

Entamoeba histolytica possesses a unique set of FYVE domain-containing proteins. Eleven out of 12 EhFP proteins have an identical modular structure consisting of RhoGEF/DH, PH and FYVE domains. Man possesses at least 27 FYVE domain-containing proteins, categorized into 14 groups (Stenmark *et al.*, 2002). A search of the NCBI non-redundant database revealed that 38 proteins possess this particular modular structure: 11 from *E. histolytica* and 27 from other organisms including 5 from *H. sapiens* and 4 from *D. discoideum*. Thus, although this modular structure is conserved in a wide range of organisms from fungi and protists to mammals, the expansion of this protein family in *E. histolytica* is striking and may reflect the reliance and complexity of PtdIns-mediated cellular signalling and network in *E. histolytica*.

A putative homologue of the amoebic RhoGEF-containing EhFPs in mammals may be FGD1, a genetic defect of which was shown to be responsible for faciogenital dysplasia (FGDY). FGD1, consisting of proline-rich, RhoGEF/DH, two PH and FYVE domains (Pasteris *et al.*, 1994), localizes to the Golgi apparatus and the cytoplasm and possesses GEF activity towards Cdc42 (Estrada *et al.*, 2001). The localization of FDG3 mutants lacking individual domains (Pasteris *et al.*, 2000) was unchanged, suggesting that the localization of FDG is

determined by an unidentified domain or redundant domain interactions. In addition, all known mutations of FGD1 in clinical cases of FGDY reside in the RhoGEF/DH or PH domain (Orrico *et al.*, 2000), suggesting the importance of these domains for intracellular targeting and/or activity of FGD1. Recently, dual targeting of FGD2 to early endosomes and membrane ruffles was reported. The FYVE domain was necessary for the targeting of FGD2 to early endosomes (Huber *et al.*, 2008). These data reinforce the importance of the FYVE domain for the recruitment of various proteins via the interaction with PtdIns(3)P. While direct binding of FGD2-FYVE with PtdIns(3)P was not demonstrated, full-length FGD2 recombinant protein was shown to bind to PtdIns(5)P, PtdIns(4,5)P2, PtdIns(3,4,5)P3 and very weakly to PtdIns(3)P. FGD2 FYVE domain was shown to determine the localization of RhoGEF/DH.

Phospholipid specificity of EhFP4 explains distinct localization of Hrs–FYVE and EhFP4 on the phagosome

Although both GFP–Hrs–FYVE and EhFP4 are recruited to the phagosome and the phagosome-associated thread-like structure during phagocytosis, their precise localizations and kinetics of recruitment differed. GFP–Hrs–FYVE was recruited to the entire membrane of phagosomes indiscriminately, while HA-EhFP4 and GFP–EhFP4–FYVE were restricted to the proximal portion of phagosomes and the tunnel-like structure. Phospholipid binding assay revealed that EhFP4 preferentially bound to PtdIns(4)P (Fig. 4B). This finding nicely explains the differential localization and kinetics of GFP–Hrs–FYVE and HA-EhFP4/GFP–EhFP4–FYVE. EhFP4 may be excluded from the distal portion of phagosomes due to the presence of other EhFP protein(s) with affinity to PtdIns(3)P on the phagosome. It is also possible that EhFP4 interacts with unidentified upstream and downstream effectors, which affect its localization.

Furthermore, we showed that the interaction of EhFP4 with PtdIns(3)P, PtdIns(4)P and PtdIns(5)P was not primarily mediated by the FYVE domain, but dependent on the previously unknown CT region (Fig. 4B). The finding that EhFP4-FYVE is not primarily involved in the phospholipid binding was unexpected because all amino acid residues shown to be critical for the PtdIns(3)P binding of EEA1 (Stenmark *et al.*, 2002) are totally conserved in the EhFP4 FYVE domain and GFP–EhFP4–FYVE showed an indistinguishable localization from HA-EhFP4FL. One may argue that dimerization of the FYVE domain is required for the PtdIns(3)P binding (Stenmark *et al.*, 2002). However, the GST fusion protein containing two tandem copies of the FYVE domains of EhFP4, which was expressed in a good yield as a soluble form, also failed to bind PtdIns(3)P, while Hrs–FYVE showed robust PtdIns(3)P-specific binding in the same context (Nakada-Tsukui, unpubl. data and Fig. 4B).

We further showed that the mutations of two conserved amino acids of the FYVE domain altered the phospholipid specificities and enhanced the binding of EhFP4 to PtdIns(3)P and PtdIns(5). Altogether, the EhFP4 FYVE domain likely modulates the phospholipid binding specificity of EhFP4 by either changing the structure of the CT domain or recruiting other protein(s). It remains unexplained how GFP–EhFP4–FYVE, which does not directly bind to phospholipids, localizes to the phagocytic cup, but it is possible that it may be recruited by binding with the endogenous EhFP4 (maybe by binding to the CT domain) or by interacting with other molecules that define its recruitment to the phagocytic cup. In both cases, the dominant negative effect of the GFP–EhFP4–FYVE expression on CHO cell phagocytosis (Fig. 6) may be due to the competition of endogenous EhFP4 or its binding partner(s) that define the localization of endogenous EhFP4 with overxpressed GFP–EhFP4–FYVE. This model needs to be tested in the future.

Specific involvement of EhFP4 and its downstream effectors in phagocytosis

Among four EhFPs examined in the present study, only EhFP4, but not EhFP1, EhFP2 or EhFP5, was involved in phagocytosis *per se*. Since EhFP2, 9 and 10 were previously detected in the phagosome proteome (Marion *et al.*, 2005; Okada *et al.*, 2006), HA-EhFP2 was expected to be associated with phagosomes. EhFP2 was detected in the phagosome proteome with 2.8 m latex beads coated with human serum (Marion *et al.*, 2005). Therefore, the recruitment of EhFP2 may be dependent on a ligand on the ingested materials. As shown in the present study, the kinetics and morphology of CHO cell phagocytosis is clearly different from bead internalization. As we did not further examine the localization of endogenous EhFP1, 2 and 5 with native antibodies, we were unable to rule out the possibility that the recruitment of these proteins may be perturbed by the amino-terminal HA-tag.

Although we were unable to show RhoGEF activity of recombinant EhFP4, which is often difficult to demonstrate with recombinant protein in other systems also (Crespo *et al.*, 1997), specific interaction of recombinant EhFP4 with EhRacC, EhRacD, 87.m00159, and 46.m00231 has been demonstrated (Fig. 5B). Our failure to demonstrate RhoGEF activity of recombinant EhFP4 may due to lack of post-translational modifications, e.g. phosphorylation as demonstrated to be important in other organisms (Crespo *et al.*, 1997; Schuebel *et al.*, 1998; Suzuki *et al.*, 2003). We have also shown the colocalization of EhFP4 and F-actin (Fig. 2D). Taken together, these results are consistent with the premise that EhFP4 is likely

one of the RhoGEF/DH proteins that interact with and activate these Rho/Rac molecules leading to actin re-arrangement during phagocytosis. Truncated EhFP4 lacking the FYVE domain and CT domain also weakly bound to three additional Rho/Rac: RacA, 140.m00084 and 69.m00185 (K. Nakada-Tsukui, unpublished), which may indicate that the substrate specificity is also attributable in part to the FYVE as well as the RhoGEF/DH domain.

To date three Dbl family RhoGEF molecules were characterized from *E. histolytica* (Aguilar-Rojas *et al.*, 2005; Arias-Romero *et al.*, 2007; Gonzalez De la Rosa *et al.*, 2007). It has been shown that EhGEF1 and EhGEF2 activate EhRacG, while EhGEF3 activates EhRacA and EhRho1 *in vitro*. EhRacA, EhRacG and EhGEF2 were previously shown to be involved in erythrophagocytosis (Ghosh and Samuelson, 1997; Guillen *et al.*, 1998; Marion *et al.*, 2005; Gonzalez De la Rosa *et al.*, 2007). Thus, the lack of interaction of EhFP4 with EhRacA and EhRacG may indicate that *E. histolytica* possesses multiple signalling pathways regulated by RhoGEFs leading to cytoskeletal re-arrangement during phagocytosis.

Among other proteins shown to be involved in phagocytosis, i.e. p21 activated kinase PAK, and calcium binding protein EhCaBP1 (Labruyere *et al.*, 2003; Jain *et al.*, 2008), we showed partial colocalization of EhCaBP1 and EhFP4. EhCaBP1 associated with the phagocytic cup only for 12 s in the very early phase of phagocytosis (Jain *et al.*, 2008). Together with the restricted colocalization of EhFP4 and EhCaBP1 at the proximal region of the phagocytic cup, these data suggest major differences in the localization and kinetics between EhFP4 and EhCaBP1. Although we were not able to monitor the kinetics of EhFP4 recruitment to the phagocytic cup in a time-lapse imaging in this study, the fact that EhFP4 was also found at the distal region of the phagocytic cups suggests that the dissociation of EhCaBP1 from the phagocytic cup precedes that of EhFP4.

Differential effects of the FYVE domain from amoebic EhFP4 and mammalian Hrs on CHO cell phagocytosis

As shown in Fig. 6, overexpression of EhFP4-FYVE repressed CHO cell phagocytosis while Hrs–FYVE enhanced it. While the inhibitory effect by EhFP4-FYVE can be explained as a competition with endogenous EhFP4, the positive effect of Hrs–FYVE on phagocytosis appears to be puzzling. It has been shown that expression of GFP fused with FYVE domain causes enlargement of endosomes (Gillooly *et al.*, 2000; Chuang *et al.*, 2007). Expression of the FYVE domain dissociates endogenous SARA (Smad anchor for receptor activation) from the rhodopsin-laden vesicles and elicits a dominant negative effect on the phospholipid-directed vesicular trafficking of rhodopsin to the outer segment, light-sensing organelle, of the vertebrate rod photoreceptor (Chuang *et al.*, 2007). These reports suggest that overexpression of FYVE domain caused dominant negative effect on PtdIns(3)P signalling. It has also been shown that inhibition of PtdIns(3)P production by wortmannin repressed RBC phagocytosis and endocytosis in *E. histolytica* (Ghosh and Samuelson, 1997). Thus, our finding that expression of GFP–Hrs–FYVE enhanced CHO cell phagocytosis in *E. histolytica* was unexpected.

There are a few possible explanations for the enhancement of CHO cell phagocytosis by Hrs–FYVE. First, GFP–Hrs–FYVE may immobilize PtdIns(3)P on the site of internalization (the phagocytic cup), and constitutively activate downstream Rho/Rac effectors via recruitment of unidentified EhFP. Second, GFP–Hrs–FYVE may perturb normal PtdIns(3)P metabolism, e.g. by inhibiting dephosphorylation of PtdIns(3)P, which results in accumulation of PtdIns(3)P. Although our finding of the enhancement of phagocytosis by GFP–Hrs–FYVE appears to contradict with the previous study where RBC phagocytosis and endocytosis were inhibited by wortmannin (Ghosh and Samuelson, 1997), the negative effects of wortmannin on phagocytosis could be attributable to other PtdIns signalling cascades because wortmannin is known to affect not only type III PI3K but also other kinds of lipid kinases (Wymann and Pirola, 1998; Oude Weernink *et al.*, 2004).

Opposite effects of the Hrs–FYVE domain on bead and CHO cell phagocytosis

While expression of GFP–Hrs–FYVE enhanced CHO cell phagocytosis (Fig. 6), it repressed phagocytosis of carboxylated beads. This observation clearly indicates that molecular mechanisms of phagocytosis of mammalian cells and negatively charged beads are different. Marion *et al.* (2005) reported remarkable differences in the protein profiles between phagosomes isolated using non-coated latex beads and those with human serum-coated beads. Taken together, these data suggest that PtdIns signals and pathways for phagocytosis are differentially triggered and transduced depending on targets to be ingested. We often observed that an *E. histolytica* trophozoite adhered to CHO cells but not internalize them. Such a trophozoite often appears to start internalization when initiated by contact with another amoeba trophozoite (K. Nakada-Tsukui, unpublished). However, we have not yet identified the signals from the neighbouring trophozoite that trigger internalization.

Finally, discovery and characterization of the unique molecular mechanisms of phagocytosis in parasitic protists should shed light on the evolution of this biological process, which is conserved from free-living and parasitic protists to professional phagocytes in higher eukaryotes.

Experimental procedures

Cells and reagents

Trophozoites of *E. histolytica* strain HM-1:IMSS cl6 (Diamond *et al.*, 1972) were maintained axenically in Diamond's BI-S-33 medium (Diamond *et al.*, 1978) at 35.5°C. Amoeba transformants were cultured in the presence of 10 or 40 g ml $^{-1}$ Geneticin (Invitrogen, San Diego, CA). Chinese hamster ovary cell lines (CHO) were maintained in F12 medium (Invitrogen, San Diego, CA) supplied with 10% fetal calf serum (MBL, Nagoya, Japan) at 37°C with 5% CO_2. Promastigotes of GFP-expressing *Leishmania amazonensis* (Chan *et al.*, 2003), a gift from Dr K. P. Chang, Rosalind Franklin University, and Dr S. Kawazu, OUAVM, were cultured in 199 medium (Nissui Pharmaceutical, Tokyo, Japan) supplemented with 10% heat-inactivated fetal calf serum, 25 mM Hepes and 5 mg ml $^{-1}$ tunicamycin at 26°C. *Escherichia coli* strain DH5 was purchased from Life Technologies (Tokyo, Japan). All chemicals of analytical grade were purchased from Sigma-Aldrich (Tokyo, Japan) unless otherwise stated.

Plasmid construction

Standard techniques were used for routine DNA manipulation, subcloning and plasmid construction as previously described (Sambrook, 2001). To produce recombinant full-length or partial proteins of EhFP4, a full-length EhFP4, a region containing DH and PH domains (aa 1–333), or a region containing DH domain only (aa 1–266) was PCR-amplified and subcloned into pColdTF vector (Takara, Tokyo Japan) and expressed as Histidine tag-trigger factor (TF)-fused recombinant protein (TF–EhFP4FL, TF–EhFP4DH–PH or TF–EhFP4–DH respectively). Two EhFP4 full-length variants containing two or one mutation, His365Ser/His366Ser (HS) and Cys375Ser (CS) mutants, were generated by PCR-based site-directed mutagenesis. Addition of TF significantly improved solubility of both full-length and truncated forms of recombinant EhFP4. Since we failed to generate soluble GST-fused full-length EhFP4, TF-fused recombinant protein was used in the binding experiments. To produce GST-fused small GTPases, the open reading frames of 108.m00133 (EhRacC; Lohia and Samuelson, 1993), 52.m00167 (EhRho1; Lohia and Samuelson, 1996), 140.m00084, 146.m00106 (EhRacG; Guillen *et al.*, 1998), 16.m00303 (EhRacD; Lohia and Samuelson, 1993), 197.m00080 (EhRacA; Lohia and Samuelson, 1993), 296.m00051, 87.m00159, 46.m00231 and 69.m00185 were PCR-amplified and subcloned into pGEX6p-2 vector (GE Healthcare UK, Buckinghamshire, UK). GST–EhRab7A was prepared as previously described (Nozaki *et al.*, 1998). To produce GST-fused partial EhFP4 proteins, FYVE or carboxyl-terminal (CT) domain (aa 321–422 and 407–495, respectively) was PCR-amplified and subcloned into pGEX6p-2.

We constructed vectors to express either a protein with three tandem copies of the influenza virus haemagglutinin (HA) epitopes at the amino terminus, or a fusion protein with three tandem copies of the c-myc (Myc) epitope followed by RFP at the amino terminus. These plasmids were designated as pEhExHA and pKT-MR respectively. The pEhExHA vector was generated by the insertion of annealed oligonucleotides corresponding to three tandem copies of the HA epitope flanked by 5′ BglII site and 3′ SmaI and XhoI sites into the BglII-XhoI site of pEhEx (Nozaki *et al.*, 1998). RFP protein coding region was PCR-amplified using pRSETB-mRFP, a gift from Dr A. Miyawaki, Riken, as a template, with SmaI and XhoI restriction sites, and subcloned into pKT-M (Saito-Nakano *et al.*, 2004) to generate pKT-MR. To develop amoeba lines expressing Myc-GFP or Myc-RFP fused with two tandem copies of the FYVE domain of Hrs, plasmids were constructed by inserting a fragment containing the Hrs-2xFYVE PCR-amplified from pEGFP-2xFYVE, a gift from Dr Tamotsu Yoshimori, Osaka Univ., into pKT-MG and pKT-MR, to generate pKT-MG-Hrs–FYVE and pKT-MR-Hrs–FYVE respectively. The same fragment was used to generate a plasmid for expressing GST-fused Hrs-2xFYVE recombinant protein by inserting the fragment into to the pGEX6p-2 vector (pGEX6p-2-Hrs–FYVE). The FYVE domain of EhFP4 (aa 333–407) was PCR-amplified and two tandem copies of the domain were subcloned into pKT-MG to produce pKT-MG-EhFP4-FYVE. To generate a vector that would express HA-EhFP fusion proteins in the amoeba, the protein coding regions of EhFP1, 2, 4 and 5 were amplified from an *E. histolytica* cDNA library using appropriate primers, designed based on nucleotide sequences found in the *E. histolytica* genome database (http://www.tigr.org/tdb/e2k1/eha1), with recognition sites for restriction enzymes. The PCR products were cloned into SmaI-XhoI site of pEhExHA vector and were designated as pEhExHA-EhFP1, 2, 3 and 5 respectively.

Amoeba transformation

Plasmids were introduced into the amoeba trophozoites by lipofection as previously described (Nozaki *et al.*, 1999). Geneticin (G418) was added, 24 h after transfection, at a concentration of 1 g ml $^{-1}$, and increased gradually for approximately 2 weeks until the drug concentration reached 40 g ml $^{-1}$ for the pKT-MG, pKT-MG-Hrs–FYVE, pKT-MG-EhFP4-FYVE, pKT-MR and pKT-MR-Hrs–FYVE transformants, and 10 g ml $^{-1}$ for the pEhExHA-EhFP transformants.

Assays for EhFP4-Rho/Rac binding and Rho guanine nucleotide exchange activity

Approximately 15 g of GST–Rho/Rac, GST–Rab7A or GST recombinant protein was mixed with 20 l of glutathione-Sepharose resin (50% suspension), and incubated at 4°C on a rocking platform for 2 h. After the GST–Rho/Rac-bound resin was incubated with EDTA buffer (10 mM EDTA, 20 mM Hepes pH 7.5, 100 mM NaCl and 1 mM DTT) to remove guanine nucleotides, the resin was incubated with 15 g of TF–EhFP4FL, TF–EhFP4DH–PH or TF in binding buffer (50 mM Hepes pH 7.5, 10 mM MgCl2, 1 mM EDTA, 1 mM DTT, and 0.05% Triton X-100) at 4°C for 16 h. Unbound proteins ('unbound') were collected, and the resin washed extensively with binding buffer. The bound proteins were dissociated from the resin by adding SDS-PAGE sample buffer ('pull-down'). The 'unbound' and 'pull down' fractions were subjected to SDS-PAGE and immunoblot with anti-His monoclonal antibody (Cell Signaling Technology, Danvers, MA, USA) or anti-GST polyclonal antibody (GE healthcare UK). The membranes were washed, and then incubated with alkaline phosphate-conjugated anti-mouse IgG (Cell Signaling Technology) or anti-rabbit IgG (Jackson Laboratory, Main, USA) for 1 h. Proteins were visualized by AP Conjugate Substrate Kit (Bio-Rad, Hercules, CA, USA).

RhoGEF activities of the EhFP4FL, EhFP4 DH-PH, EhFP4 DH, EhFP4FL HS and EhFP4FL CH mutants were determined

by using RhoGEF exchange assay biochem kit (BK100; cytoskeleton, Denver, CO) and human Rac1(hRac1), hCdc42, hRhoA and 146.m00106 (EhRacG), 16.m00303 (EhRacD), 140.m00084, 296.m00051, 87.m00159, 46.m00231 and 69.m00185.

Live cell imaging

Approximately 5 10^5 cells of *E. histolytica* GFP–Hrs–FYVE transformants were cultured on a 35 mm collagen-coated glass-bottom culture dish (MatTek Corporation, Ashland, MA) in 3 ml of BI-S-33 medium under anaerobic conditions. CHO cells were stained for 30 min with 20 M Cell tracker blue dye or Cell tracker orange dye (Molecular probes, Eugene, OR) in F12 medium containing 10% FCS. After staining, CHO cells were washed three times with fresh BI-S-33 medium, and approximately 2 10^5 CHO cells in 200 l BI-S-33 medium were added to the GFP–Hrs–FYVE expressing amoeba in a glass-bottom dish. The culture was carefully covered with a coverslip, and overloaded medium was removed. The junction of the coverslip and slide glass was sealed with nail polish, and the culture was incubated at 35°C in a temperature control unit on an AS Multi Dimension Workstation (AS-MDW, Leica Microsystems, Wetzlar, Germany) equipped with a 63 /NA 1.30 oil immersion objective and CCD camera (Coolsnap HQ, Roper Scientific, Duluth, GA). Fluorescence images of 59 continuous slices (z-stack) with 0.5 m intervals were obtained every 20 s with the BGR filter at excitation wavelengths 492.3 nm for GFP and 389.9 nm for Cell tracker blue.

For confocal microscopic analysis, the culture was incubated at 38°C on the heating insert of Zeiss LSM510 META (Carl-Zeiss microimaging, Jena, Germany) equipped with a 63 /NA 1.4 oil immersing objective with a piezo controller. GFP was excited with the 488 nm laser line of an argon laser with a 505–530 nm filter for emission. Cell tracker orange was excited with the 543-nm line of a HeNe laser, with a 560-nm long pass filter for emission. In Video S1, images were taken every 1 s, while in Video S2, images of 11 slices with 2 m intervals were obtained every 10 s. The profile of GFP–Hrs–FYVE signal on a nascent phagosome, shown in Video S1, was analysed using the *profile tool* in the LSM software.

*Measurement of phagosome pH and degradation of GFP–*L. amazonensis

Phagosome pH and degradation of GFP–*L. amazonensis* in RFP and RFP-FYVE-overexpressing *E. histolytica* transformants were measured as previously described (Mitra *et al.*, 2005).

Production of Anti-EhFP4 antibody

Anti-EhFP4 antiserum was generated by immunizing two guinea pigs with TF-EhFP4 FL recombinant protein at Kitayama Rabes, Nagano, Japan.

Indirect immunofluorescence assay

Indirect immunofluorescence assay was performed as previously described (Saito-Nakano *et al.*, 2004) with some modifications. Briefly, amoeba transformant cells expressing GFP–Hrs–FYVE, GFP–EhFP4–FYVE, HA-EhFP1, 2, 4 or 5 were harvested and transferred to 8 mm round wells on a slide glass. CHO cells were prestained with 10 M of Cell tracker orange or 20 M of Cell tracker green (Molecular Probes, Eugene, OR) for 30 min, harvested, and washed with BI-S-33 medium. Approximately 1.5 10^5 amoebae were incubated with 1.5 10^5 of Cell tracker-stained CHO cells for the times indicated, and after washing, fixed with 3.7% paraformaldehyde in phosphate buffered saline (PBS), pH 7.2 for 10 min. The amoebae and CHO cells were washed and then permeabilized with 0.2% saponin in PBS containing 1% BSA for 10 min, and reacted with a primary antibody diluted at 1:1000 (anti-HA monoclonal antibody, 11MO, Covance, Princeton, NJ), 1:500 (anti-EhFP4 antiserum), or 1:100 (anti-EhCaBP1 antiserum) in PBS containing 0.2% saponin and 1% BSA. After washing, the samples were then incubated with Alexa Fluor 488-, 568- or 633- conjugated anti-rabbit, anti-mouse, or anti-guinea pig secondary antibody (1:1000) for 1 h. For phallacidin staining, fixed and permeabilized trophozoites were incubated with 0.33 M of BODIPY FL phallacidin (Molecular Probes, Eugine, OR) for 20 min. The samples were examined on a Carl-Zeiss LSM 510 META confocal laser-scanning microscope, and images were analysed using LSM510 software.

DNA microarray

A custom short oligonucleotide microarray was fabricated by Virginia Bioinformatics Institute, Blacksburg, VA with a license from Affymetrix (Santa Clara, CA, USA) as previously described (Gilchrist *et al.*, 2006). These arrays were designed with probes targeting both predicted mRNAs (9435 of the 9938 predicted genes) and intergenic regions. Total RNA from three independent cultures, isolated as previously described (Gilchrist *et al.*, 2006), were used to generate expression profiles, which showed a correlation coefficient greater than 0.95, indicating that the result was reproducible. Data were further analysed with the GCOS software (Affymetrix, Santa Clara, CA, USA). Detailed analysis of the microarray data will be presented elsewhere.

Phosphoinositide binding assay

Nitrocellulose membranes with spotted various phosphoinositides and other lipids (PIP strips) were purchased from Echelon Research Laboratories (Salt Lake City, UT). Membranes were blocked with 1% skim-milk in PBS for 1 h at room temperature. Blocked membranes were incubated overnight at 4°C with 10 g ml ^{1} TF, TF–EhFP4FL, TF-EhFP4 DH-PH, TF-EhFP4 DH, TF–EhFP4FL HS and TF–EhFP4FL CS mutants, and recombinant proteins GST–EhFP4–FYVE and GST–EhFP4–CT. The membranes were then washed three times for 10 min in PBS containing 0.1% tween-20. The membranes were incubated with anti-His monoclonal antibody (1:500 dilution, Cell Signaling Technology) or anti-GST polyclonal antibody (1:500 dilution, GE healthcare UK), for 1 h at room temperature followed by washing. The membranes were incubated with HRP-conjugated anti-mouse secondary antibody (1:500 dilution) or alkaline phosphatase (AP)-conjugated anti-goat secondary antibody (1:1000 dilution) for 1 h at room temperature. After washing, the proteins were detected by chemiluminescence as described above (for HRP-conjugated secondary antibody) or with an AP conjugate substrate kit (Bio-Rad, Hercules, CA) (for AP-conjugated secondary antibody).

Phagocytosis assay

Approximately 10^5 amoebae were grown overnight in a 24-well plate under anaerobic conditions. Roughly 4–8 10^5 of Cell tracker orange-loaded CHO cells or 5 l of Nile Red fluorescent carboxylate-modified FluoSphere microspheres (Molecular Probes, Eugene, OR) was added to the amoeba, and incubated for 0, 10, 30 or 60 min. After incubation, the amoebae were washed once with warm PBS containing 250 mM galactose (PBS-galactose), and 450 l of PBS-galactose was added. The plate was chilled on ice and detached amoebae were recovered and analysed by two-colour flow cytometry (FACSCalibur, BD, Franklin Lakes, NJ).

Accession numbers

The nucleotide sequence data reported in this paper are available in the DDBJ/GenBank/EBI databases with the following accession numbers: EhFP1, XP_651719; EhFP2, XP_655361; EhFP3, XP_650743; EhFP4, XP_656365; EhFP5, XP_649382; EhFP6, XP_651964; EhFP7, XP_654401; EhFP8, XP_651711; EhFP9, XP_656765; EhFP10, XP_651436;EhFP11, XP_651674; EhFP12, XP_656065; 108.m00133, EHI_070730, XP_652693; 52.m00167, EHI_029020, XP_654488; 140.m00084, XP_651936; 146.m00106, EHI_129750, XP_651800; 16.m00303, EHI_012240, XP_656184; 197.m00080, EHI_197840, XP_650831; 296.m00051, EHI_135450, XP_649502; 87.m00159, EHI_146180, XP_653308; 46.m00231, EHI_194390, XP_654700; 69.m00185, EHI_192450, XP_653885

Acknowledgements

We thank Alok Bhattacharya, Jawaharal Nehru University, for EhCaBP1 antibody, Miguel Vargas, CINVESTAV, for EhGEF1 and EhRacG construct, Gil Penuliar for proof reading the manuscript, Yoko Yamada, Tomoko Akuzawa, Atsushi Furukawa, Mai Nudejima, Fumie Tokumaru, and Yasuo Shigeta for technical assistance. This work was supported by the Grant-in-Aid for Scientific Research from the Ministry of Education, Culture, Sports, Science and Technology of Japan awarded to T.N. (18050006, 18073001, 18GS0314, 20390119) and K.N.T. (18790291, 20790323), a grant for Research on Emerging and Re-emerging Infectious Diseases from the Ministry of Health, Labour, and Welfare (H20-Shinkosaiko-Ippan-016), and a grant for research to promote the development of anti-AIDS pharmaceuticals from the Japan Health Sciences Foundation awarded to T.N.

References

Ackers, J.P., and Mirelman, D. (2006) Progress in research on *Entamoeba histolytica* pathogenesis. *Curr Opin Microbiol* 9: 367–373.

Aguilar-Rojas, A., de Jesus Almaraz-Barrera, M., Krzeminski, M., Robles-Flores, M., Hernandez-Rivas, R., Guillen, N., *et al.* (2005) *Entamoeba histolytica*: inhibition of cellular functions by overespression of EhGEF1, a novel Rho/Rac guanine nucleotide exchange factor. *Exp Parasitol* 109: 150–162.

Arias-Romero, L.E., de Jesus Almaraz-Barrera, M., Diaz-Valencia, J.D., Rojo-Dominguez, A., Hernandez-Rivas, R., and Vargas, M. (2006) EhPAK2, a novel p21-activated kinase, is required for collagen invasion and capping in *Entamoeba histolytica*. *Mol Biochem Parasitol* 149: 17–26.

Arias-Romero, L.E., Gonzalez de la Rosa, C.H., de Jesus Almaraz-Barrera, M., Diaz-Valencia, J.D., Sosa-Peinado, A., and Vargas, M. (2007) EhGEF3, a novel Dbl family member, regulates EhRacA activation during chemotaxis and capping in *Entamoeba histolytica*. *Cell Motil Cytoskeleton* 64: 390–404.

Balla, T. (2005) Inositol-lipid binding motifs: signal integrators through protein-lipid and protein–protein interactions. *J Cell Sci* 118: 2093–2104.

Botelho, R.J., Scott, C.C., and Grinstein, S. (2004) Phosphoinositide involvement in phagocytosis and phagosome maturation. *Curr Top Microbiol Immunol* 282: 1–30.

Burd, C.G., and Emr, S.D. (1998) Phosphatidylinositol (3) -phosphate signaling mediated by specific binding to RING FYVE domains. *Mol Cell* 2: 157–162.

Chan, M.M., Bulinski, J.C., Chang, K.P., and Fong, D. (2003) A microplate assay for *Leishmania amazonensis* promastigotes expressing multimeric green fluorescent protein. *Parasitol Res* 89: 266–271.

Chua, J., and Deretic, V. (2004) *Mycobacterium tuberculosis* reprograms waves of phosphatidylinositol 3-phosphate on phagosomal organelles. *J Biol Chem* 279: 36982–36992.

Chuang, J.Z., Zhao, Y., and Sung, C.H. (2007) SARA-regulated vesicular targeting underlies formation of the light-sensing organelle in mammalian rods. *Cell* 130: 535–547.

Clark, C.G., Alsmark, U.C., Tazreiter, M., Saito-Nakano, Y., Ali, V., Marion, S., *et al.* (2007) Structure and content of the *Entamoeba histolytica* genome. *Adv Parasitol* 65: 51–190.

Coudrier, E., Amblard, F., Zimmer, C., Roux, P., Olivo-Marin, J.C., Rigothier, M.C., and Guillen, N. (2005) Myosin II and the Gal-GalNAc lectin play a crucial role in tissue invasion by *Entamoeba histolytica*. *Cell Microbiol* 7: 19–27.

Crespo, P., Schuebel, K.E., Ostrom, A.A., Gutkind, J.S., and Bustelo, X.R. (1997) Phosphotyrosine-dependent activation of Rac-1 GDP/GTP exchange by the vav proto-oncogene product. *Nature* 385: 169–172.

Diamond, L.S., Mattern, C.F., and Bartgis, I.L. (1972) Viruses of *Entamoeba histolytica*. I. Identification of transmissible virus-like agents. *J Virol* 9: 326–341.

Diamond, L.S., Harlow, D.R., and Cunnick, C.C. (1978) A new medium for the axenic cultivation of *Entamoeba histolytica* and other *Entamoeba*. *Trans R Soc Trop Med Hyg* 72: 431–432.

Ehrenkaufer, G.M., Haque, R., Hackney, J.A., Eichinger, D.J., and Singh, U. (2007) Identification of developmentally regulated genes in *Entamoeba histolytica*: insights into mechanisms of stage conversion in a protozoan parasite. *Cell Microbiol* 9: 1426–1444.

Ellson, C.D., Anderson, K.E., Morgan, G., Chilvers, E.R., Lipp, P., Stephens, L.R., and Hawkins, P.T. (2001) Phosphatidylinositol 3-phosphate is generated in phagosomal membranes. *Curr Biol* 11: 1631–1635.

Estrada, L., Caron, E., and Gorski, J.L. (2001) Fgd1, the Cdc42 guanine nucleotide exchange factor responsible for faciogenital dysplasia, is localized to the subcortical actin cytoskeleton and Golgi membrane. *Hum Mol Genet* 10: 485–495.

Franco-Barraza, J., Zamudio-Meza, H., Franco, E., del Carmen Dominguez-Robles, M., Villegas-Sepulveda, N., and Meza, I. (2006) Rho signaling in *Entamoeba histolytica* modulates actomyosin-dependent activities stimulated during invasive behavior. *Cell Motil Cytoskeleton* 63: 117–131.

Fratti, R.A., Backer, J.M., Gruenberg, J., Corvera, S., and Deretic, V. (2001) Role of phosphatidylinositol 3-kinase and Rab5 effectors in phagosomal biogenesis and mycobacterial phagosome maturation arrest. *J Cell Biol* 154: 631–644.

Frederick, J.R., and Petri, W.A., Jr (2005) Roles for the galactose-/N-acetylgalactosamine-binding lectin of *Entamoeba* in parasite virulence and differentiation. *Glycobiology* 15: 53R–59R.

Gaullier, J.M., Simonsen, A., D'Arrigo, A., Bremnes, B., Stenmark, H., and Aasland, R. (1998) FYVE fingers bind PtdIns(3)P. *Nature* 394: 432–433.

Ghosh, S.K., and Samuelson, J. (1997) Involvement of p21racA, phosphoinositide 3-kinase, and vacuolar ATPase in phagocytosis of bacteria and erythrocytes by *Entamoeba histolytica*: suggestive evidence for coincidental evolution of amebic invasiveness. *Infect Immun* 65: 4243–4249.

Gilchrist, C.A., Houpt, E., Trapaidze, N., Fei, Z., Crasta, O., Asgharpour, A., *et al.* (2006) Impact of intestinal colonization and invasion on the *Entamoeba histolytica* transcriptome. *Mol Biochem Parasitol* 147: 163–176.

Gillooly, D.J., Morrow, I.C., Lindsay, M., Gould, R., Bryant, N.J., Gaullier, J.M., *et al.* (2000) Localization of phosphatidylinositol 3-phosphate in yeast and mammalian cells. *EMBO J* 19: 4577–4588.

Gillooly, D.J., Simonsen, A., and Stenmark, H. (2001) Cellular functions of phosphatidylinositol 3-phosphate and FYVE domain proteins. *Biochem J* 355: 249–258.

Gonzalez De la Rosa, C.H., Arias-Romero, L.E., de Jesus Almaraz-Barrera, M., Hernandez-Rivas, R., Sosa-Peinado, A., Rojo-Dominguez, A., *et al.* (2007) *Eh*GEF2, a DblRhoGEF from *Entamoeba histolytica* has atypical biochemical properties and participates in essential cellular process. *Mol Biochem Parasitol* 151: 70–80.

Guillen, N., Boquet, P., and Sansonetti, P. (1998) The small GTP-binding protein RacG regulates uroid formation in the protozoan parasite *Entamoeba histolytica*. *J Cell Sci* 111 (Pt 12): 1729–1739.

Halet, G. (2005) Imaging phosphoinositide dynamics using GFP-tagged protein domains. *Biol Cell* 97: 501–518.

Haque, R., Mondal, D., Kirkpatrick, B.D., Akther, S., Farr, B.M., Sack, R.B., and Petri, W.A., Jr (2003) Epidemiologic and clinical characteristics of acute diarrhea with emphasis on *Entamoeba histolytica* infections in preschool children in an urban slum of Dhaka, Bangladesh. *Am J Trop Med Hyg* 69: 398–405.

Huber, C., Mårtensson, A., Bokoch, G.M., Nemazee, D., and Gavin, A.L. (2008) FGD2, aCDC42-specific exchange factor expressed by antigen-presenting cells, localizes to early endosomes and active membrane ruffles. *J Biol Chem* 283: 34002–34012.

Jain, R., Santi-Rocca, J., Padhan, N., Bhattacharya, S., Guillen, N., and Battacharya, A. (2008) Calcium-binding protein 1 of *Entamoeba histolytica* transiently associates with phagocytic cups in a calcium-independent manner. *Cell Microbiol* 10: 1373–1389.

Komada, M., Masaki, R., Yamamoto, A., and Kitamura, N. (1997) Hrs, a tyrosine kinase substrate with a conserved double zinc finger domain, is localized to the cytoplasmic surface of early endosomes. *J Biol Chem* 272: 20538–20544.

Labruyere, E., and Guillen, N. (2006) Host tissue invasion by *Entamoeba histolytica* is powered by motility and phagocytosis. *Arch Med Res* 37: 253–258.

Labruyere, E., Zimmer, C., Galy, V., Olivo-Marin, J.C., and Guillen, N. (2003) EhPAK, a member of the p21-activated kinase family, is involved in the control of *Entamoeba histolytica* migration and phagocytosis. *J Cell Sci* 116: 61–71.

Lejeune, A., and Gicquaud, C. (1987) Evidence for two mechanisms of human erythrocyte endocytosis by *Entamoeba histolytica*-like amoebae (Laredo strain). *Biol Cell* 59: 239–245.

Lejeune, A., and Gicquaud, C. (1992) Target cell deformability determines the type of phagocytic mechanism used by *Entamoeba histolytica*-like, Laredo strain. *Biol Cell* 74: 211–216.

Lindmo, K., and Stenmark, H. (2006) Regulation of membrane traffic by phosphoinositide 3-kinases. *J Cell Sci* 119: 605–614.

Loftus, B., Anderson, I., Davies, R., Alsmark, U.C., Samuelson, J., Amedeo, P., *et al.* (2005) The genome of the protist parasite *Entamoeba histolytica*. *Nature* 433: 865–868.

Lohia, A., and Samuelson, J. (1993) Molecular cloning of a rho family gene of *Entamoeba histolytica*. *Mol Biochem Parasitol* 58: 177–180.

Lohia, A., and Samuelson, J. (1996) Heterogeneity of *Entamoeba histolytica* rac genes encoding p21rac homologues. *Gene* 173: 205–208.

Marion, S., Laurent, C., and Guillen, N. (2005) Signalization and cytoskeleton activity through myosin IB during the early steps of phagocytosis in *Entamoeba histolytica*: a proteomic approach. *Cell Microbiol* 7: 1504–1518.

Mitra, B.N., Yasuda, T., Kobayashi, S., Saito-Nakano, Y., and Nozaki, T. (2005) Differences in morphology of phagosomes and kinetics of acidification and degradation in phagosomes between the pathogenic *Entamoeba histolytica* and the non-pathogenic *Entamoeba dispar*. *Cell Motil Cytoskeleton* 62: 84–99.

Mitra, B.N., Kobayashi, S., Saito-Nakano, Y., and Nozaki, T. (2006) *Entamoeba histolytica*: differences in phagosome acidification and degradation between attenuated and virulent strains. *Exp Parasitol* 114: 57–61.

Nakada-Tsukui, K., Saito-Nakano, Y., Ali, V., and Nozaki, T. (2005) A retromerlike complex is a novel Rab7 effector that is involved in the transport of the virulence factor cysteine protease in the enteric protozoan parasite *Entamoeba histolytica*. *Mol Biol Cell* 16: 5294–5303.

Nozaki, T., Asai, T., Kobayashi, S., Ikegami, F., Noji, M., Saito, K., and Takeuchi, T. (1998) Molecular cloning and characterization of the genes encoding two isoforms of cysteine synthase in the enteric protozoan parasite *Entamoeba histolytica*. *Mol Biochem Parasitol* 97: 33–44.

Nozaki, T., Asai, T., Sanchez, L.B., Kobayashi, S., Nakazawa, M., and Takeuchi, T. (1999) Characterization of the gene encoding serine acetyltransferase, a regulated

enzyme of cysteine biosynthesis from the protist parasites *Entamoeba histolytica* and *Entamoeba dispar*. Regulation and possible function of the cysteine biosynthetic pathway in *Entamoeba*. *J Biol Chem* 274: 32445–32452.

Okada, M., Huston, C.D., Oue, M., Mann, B.J., Petri, W.A. Jr, Kita, K., and Nozaki, T. (2006) Kinetics and strain variation of phagosome proteins of *Entamoeba histolytica* by proteomic analysis. *Mol Biochem Parasitol* 145: 171–183.

Orrico, A., Galli, L., Falciani, M., Bracci, M., Cavaliere, M.L., Rinaldi, M.M., *et al.* (2000) A mutation in the pleckstrin homology (PH) domain of the FGD1 gene in an Italian family with faciogenital dysplasia (Aarskog–Scott syndrome). *FEBS Lett* 478: 216–220.

Oude Weernink, P.A., Schmidt, M., and Jakobs, K.H. (2004) Regulation and cellular roles of phosphoinositide 5-kinases. *Eur J Pharmacol* 500: 87–99.

Pasteris, N.G., Cadle, A., Logie, L.J., Porteous, M.E., Schwartz, C.E., Stevenson, R.E., *et al.* (1994) Isolation and characterization of the faciogenital dysplasia (Aarskog–Scott syndrome) gene: a putative Rho/Rac guanine nucleotide exchange factor. *Cell* 79: 669–678.

Pasteris, N.G., Nagata, K., Hall, A., and Gorski, J.L. (2000) Isolation, characterization, and mapping of the mouse Fgd3 gene, a new Faciogenital Dysplasia (FGD1; Aarskog Syndrome) gene homologue. *Gene* 242: 237–247.

Powell, R.R., Welter, B.H., Bowersox, B., Attaway, C., and Temesvari, L.A. (2006) *Entamoeba histolytica*: FYVE -finger domains, phosphatidylinositol 3-phosphate biosensors, associate with phagosomes but not fluid filled endosomes. *Exp Parasitol* 112: 221–231.

Que, X., and Reed, S.L. (2000) Cysteine proteinases and the pathogenesis of amebiasis. *Clin Microbiol Rev* 13: 196–206.

Rossman, K.L., Der, C.J., and Sondek, J. (2005) GEF means go: turning on RHO GTPases with guanine nucleotide-exchange factors. *Nat Rev Mol Cell Biol* 6: 167–180.

Saito-Nakano, Y., Yasuda, T., Nakada-Tsukui, K., Leippe, M., and Nozaki, T. (2004) Rab5-associated vacuoles play a unique role in phagocytosis of the enteric protozoan parasite *Entamoeba histolytica*. *J Biol Chem* 279: 49497–49507.

Saito-Nakano, Y., Mitra, B.N., Nakada-Tsukui, K., Sato, D., and Nozaki, T. (2007) Two Rab7 isotypes, EhRab7A and EhRab7B, play distinct roles in biogenesis of lysosomes and phagosomes in the enteric protozoan parasite *Entamoeba histolytica*. *Cell Microbiol* 9: 1796–1808.

Sambrook, J.A.R., and Russell, D.W. (2001) *Molecular Cloning*. Cold Spring Harbor, NY: Cold Spring Harbor Laboratory Press.

Schuebel, K.E., Movilla, N., Rosa, J.L., and Bustelo, X.R. (1998) Phosphorylation-dependent and constitutive activation of Rho proteins by wild-type and oncogenic Vav-2. *EMBO J* 17: 6608–6621.

Scott, C.C., Dobson, W., Botelho, R.J., Coady-Osberg, N., Chavrier, P., Knecht, D.A., *et al.* (2005) Phosphatidylinositol-4,5-bisphosphate hydrolysis directs actin remodeling during phagocytosis. *J Cell Biol* 169: 139–149.

Stenmark, H., Aasland, R., Toh, B.-H., and D'Arrigo, A. (1996) Endosomal localization of the autoantigen EEA1 is mediated by a zinc-binding FYVE finger. *J Biol Chem* 271: 24048–24054.

Stenmark, H., Aasland, R., and Driscoll, P.C. (2002) The phosphatidylinositol 3-phosphate-binding FYVE finger. *FEBS Lett* 513: 77–84.

Suzuki, N., Nakamura, S., Mano, H., and Kozasa, T. (2003) Galpha 12 activates Rho GTPase through tyrosine-phosphorylated leukemia-associated RhoGEF. *Proc Natl Acad Sci USA* 100: 733–738.

Swanson, J.A., Johnson, M.T., Beningo, K., Post, P., Mooseker, M., and Araki, N. (1999) A contractile activity that closes phagosomes in macrophages. *J Cell Sci* 112 (Pt 3): 307–316.

Vargas, M., and Gonzalez-de la Rosa, C.H. (2007) Structural and functional organization of the RhoGEF proteins from *Entamoeba hisolytica*. In *Advances in the Immunobiology of Parasitic Diseases*. Terrazes, L.I. (ed.). Kerala: Research Signpost, pp. 339–359.

Vieira, O.V., Harrison, R.E., Scott, C.C., Stenmark, H., Alexander, D., Liu, J., *et al.* (2004) Acquisition of Hrs, an essential component of phagosomal maturation, is impaired by mycobacteria. *Mol Cell Biol* 24: 4593–4604.

Voigt, H., and Guillen, N. (1999) New insights into the role of the cytoskeleton in phagocytosis of *Entamoeba histolytica*. *Cell Microbiol* 1: 195–203.

Wymann, M.P., and Pirola, L. (1998) Structure and function of phosphoinositide 3-kinases. *Biochim Biophys Acta* 1436: 127–150.

Yeung, T., Ozdamar, B., Paroutis, P., and Grinstein, S. (2006) Lipid metabolism and dynamics during phagocytosis. *Curr Opin Cell Biol* 18: 429–437.

Yu, X., Lu, N., and Zhou, Z. (2008) Phagocytic receptor CED-1 initiates a signaling pathway for degrading engulfed apoptotic cells. *PLoS Biol* 6: e61.

Supporting information

Additional Supporting Information may be found in the online version of this article:

Fig. S1. Measurement of the fluorescence intensity of GFP–Hrs–FYVE on the nascent phagosome. The distribution of the signal intensity at channel 2 (green, GFP) and channel 3 (red, Cell tracker red) on the dissected plane, indicated by red arrows, were plotted using *profile tool* in the Carl Zeiss LSM510 software at two representative time points (top, 0.2 s; bottom, 165.4 s). The time kinetics of the GFP signal on the nascent phagosome is shown in Fig. 1D. Vertical black arrows indicate the region where the fluorescence signal was measured.

Fig. S2. The percentages of phagosomes (upper panel) and the phagocytic cups (lower panel) associated or not associated with GFP–Hrs–FYVE. *E. histolytica* trophozoites expressing GFP–Hrs–FYVE were co-cultured with Cell tracker blue-loaded CHO cells for 10, 30 and 60 min. The amoebae and CHO cells were fixed and examined by Zeiss LSM510. The percentages of the CHO-containing phagosomes and the phagocytic cups that were positive for GFP–Hrs–FYVE (filled bars), or negative (open bars) at indicated time points are shown. The mean and standard deviation of two independent experiments are shown.

Fig. S3. Localization of endogenous EhFP4. Anti-EhFP4 antibody was raised by immunizing guinea pigs with TF–EhFP4FL recombinant protein.

A–E. Localization of EhFP4 in the HA-EhFP4FL-expressing trophozoite. HA-EhFP4FL-expressing trophozoites were co-cultured with Cell tracker-blue-loaded CHO cells for 30 min, fixed and reacted with anti-HA and anti-EhFP4 antibody. The cells were then reacted with Alexa-568 conjugated anti-mouse IgG and Alexa-488 conjugated anti-guinea pig IgG antibody. Arrows indicate the phagocytic cup.

F–N. Localization of endogenous EhFP4 in HM-1:IMSS cl6. HM-1:IMSS cl6 trophozoites were co-cultured with CHO cells and reacted with anti-EhFP4 antibody. Arrows indicate the phagocytic cup. Bars, 10 m.

Fig. S4. Localization of wild-type EhFP4 (top) and mutant EhFP4 lacking FYVE and C-term domains (bottom) during CHO cell phagocytosis. Three additional trophozoites expressing HA-tagged wild-type EhFP4 (upper panel) or EhFP4DH-PH (lower panel) are shown. See Fig. 3A for experimental details. Arrows indicate HA-EhFP4 on the tunnel-like structure. Open arrowheads indicate structures not associated with FYVE-deficient HA-EhFP4 mutant. Bars, 10 m.

Fig. S5. Localization of GFP–Hrs–FYVE during erythrophagocytosis. *E. histolytica* trophozoites expressing GFP–Hrs–FYVE were co-cultured with gerbil erythrocytes for 40 min, fixed and examined by confocal microscopy. Arrows indicate GFP-positive phagosomes. Bars, 10 m.

Video S1. A GFP–Hrs–FYVE-expressing *E. histolytica* trophozoite ingests a Cell tracker orange-loaded CHO cell (pseudocolored in red). Images were captured every s on Zeiss LSM510 META. An *E. histolytica* trophozoite, which remains at the centre in the course of movie, ingests a CHO cell. Note that this trophozoite has already ingested another CHO cell prior to the beginning of the movie, and thus contains two phagosomes on this plane: one GFP–Hrs–FYVE-positive and one negative phagosome. This trophozoite adheres to a CHO cell (0 min), and initiates internalization (0.082 min). GFP–Hrs–FYVE starts to accumulate on the phagocytic cup (0.824 min). The entire circumference of the enclosed phagosome becomes positive for GFP–Hrs–FYVE (1.483 min). A thread-like structure connecting two phagosomes is also visible (2.801 min). An extended CHO cell being simultaneously internalized by two neighbouring trophozoites, which is typically seen in 'slow phagocytosis', is also visible (e.g. 0 min).

Video S2. This movie shows the kinetics of 'slow phagocytosis'. A GFP–Hrs–FYVE expressing-*E. histolytica* trophozoite ingests a Cell tracker orange-loaded CHO cell. Images of 11 slices with 2 m intervals were obtained every 10 s on Zeiss LSM510 META. Time series of a single representative plane are shown. A trophozoite adheres to a CHO cell (0.17 min) and starts internalization (0.33 min). The GFP–Hrs–FYVE-positive tunnel structure is visible for at least 5.17 min, supporting the continuity of 'slow phagocytosis'. Also note the PtdIns(3)P-decorated thread-like structure between the phagosome and PtdIns(3)P-positive vesicles surrounding the phagosome. Images for the first 5 min are included in the video.

Please note: Wiley-Blackwell are not responsible for the content or functionality of any supporting materials supplied by the authors. Any queries (other than missing material) should be directed to the corresponding author for the article.

IUBMB *Life*, 61(11): 1019–1028, November 2009

Critical Review

Methionine Gamma-Lyase: The Unique Reaction Mechanism, Physiological Roles, and Therapeutic Applications Against Infectious Diseases and Cancers

Dan Sato[1,2] and Tomoyoshi Nozaki[3]

[1]*Institute for Advanced Biosciences, Keio University, Tsuruoka, Yamagata, Japan*
[2]*Center for Integrated Medical Research, School of Medicine, Keio University, Shinjuku, Tokyo, Japan*
[3]*Department of Parasitology, National Institute of Infectious Diseases, Shinjuku, Tokyo, Japan*

Summary

Sulfur-containing amino acids (SAAs) are essential components in many biological processes and ubiquitously distributed to all organisms. Both biosynthetic and catabolic pathways of SAAs are heterogeneous among organisms and between developmental stages, and regulated by the environmental changes. Limited lineage of organisms ranging from archaea to plants, but not human, possess a unique enzyme methionine gamma-lyase (MGL, EC 4.4.1.11) to directly degrade SAA to α-keto acids, ammonia, and volatile thiols. The reaction mechanisms and the physiological roles of this enzyme are partially demonstrated by the enzymological analyzes, structure determination, isotopic labeling of the intermediate metabolites, and functional analyzes of deficient mutants. MGL has been exploited as a drug target for the infectious diseases caused by parasitic protozoa and anaerobic periodontal bacteria. In addition, MGL has been utilized to develop therapeutic interventions of various cancers, by introducing recombinant proteins to deplete methionine essential for the growth of cancer cells. In this review, we discuss the current understanding of enzymological properties, putative physiological roles, and therapeutic applications of MGL. © 2009 IUBMB

IUBMB *Life*, 61(11): 1019–1028, 2009

Keywords sulfur-containing amino acid; pyridoxal 5′-phosphate; protozoa; periodontal bacteria; cancer.

Abbreviations MGL, methionine gamma-lyase; SAA, sulfur-containing amino acid.

Received 19 June 2009; accepted 5 August 2009

Address correspondence to: Tomoyoshi Nozaki, Department of Parasitology, National Institute of Infectious Diseases, 1-23-1 Toyama, Shinjuku, Tokyo 162-8640, Japan. Tel: +81-3-5285-1111 ext. 2600. Fax: +81-3-5285-1219. E-mail: nozaki@nih.go.jp

ISSN 1521-6543 print/ISSN 1521-6551 online
DOI: 10.1002/iub.255

INTRODUCTION

Sulfur is an essential element in all living organisms. Bacteria and plants incorporate sulfur as inorganic compounds such as sulfate, sulfite, and sulfide. In contrast, most of heterotrophs take in sulfur as sulfur-containing amino acids (SAAs) synthesized by other organisms. SAAs play critical roles in a variety of biological processes including protein synthesis, methylation, biosynthesis of vitamins, polyamines, and antioxidants. SAAs are ubiquitously distributed, but their metabolic pathways diverged among organisms, and are modulated in the life cycle and upon stresses and changes in environmental conditions (*1*).

Both biosynthesis and degradation of SAAs (a simplified scheme is shown in Fig. 1) must be tightly regulated. The maintenance of low homocysteine concentrations is essential not only for a proper flow of sulfur in the transsulfuration pathway and the methionine cycle, but also for evading toxic effects of the molecule, which has been implicated in pathological conditions associated with various genetic disorders causing homocystinuria and homocysteinemia (*2*). Homocysteine has also been shown to be the pro-oxidant causing damage to the vascular endothelia (*3*), and associated with an increased cardiovascular risk (*4*) and Alzheimer's disease (*5*).

In mammals, SAAs are mainly degraded via oxidative cysteine catabolism, where cysteine dioxygenase (EC. 1. 13. 11. 20) catalyzes the oxygenation of cysteine to 3-sulfinoalanine, a key intermediate of cysteine metabolism leading to hypotaurine, taurine, pyruvate, and sulfate (*6*). The other cysteine degradative pathway in mammals is initiated by cysteine aminotransferase (EC. 2. 6. 1. 3), which deaminates cysteine to form 3-mercaptopyruvate. The SAA biosynthesis and degradation in mammals have recently been reviewed by Stipanuk (*2*). In the organisms that possess a methionine biosynthetic pathway, such as bacteria and plants, cystine (a pair of cysteines joined by a disulfide bond) is also degraded at least *in vitro* by cystathionine beta-lyase (EC. 4. 4. 1. 8) to thiocysteine, pyruvate, and ammonia

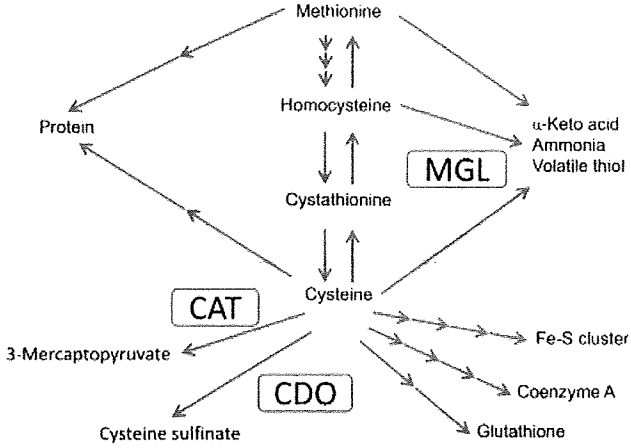

Figure 1. A general scheme of transsulfuration, methionine cycle, and sulfur-containing amino acid degradation. The enzymes involved in sulfur-containing amino acid degradation are boxed. MGL, methionine gamma-lyase; CDO, cysteine dioxygenase; CAT, cysteine aminotransferase. [Color figure can be viewed in the online issue, which is available at www.interscience.wiley.com.]

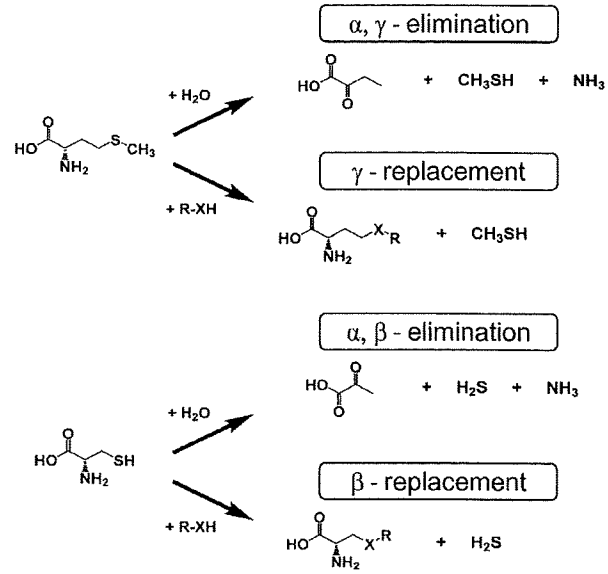

Figure 2. Catalytic reactions of MGL. α, γ-elimination and γ-replacement of L-methionine (upper) and, the α, β-elimination and β-replacement of L-cysteine (lower) are indicated. X=S or Se.

(*7*, *8*). On the other hand, a limited lineage of organisms possess the unique pathway, in which SAAs are converted to α-keto acids, ammonia, and volatile thiols by methionine gamma-lyase (MGL, EC. 4. 4. 1. 11).

Since Onitake reported 70 years ago that some bacteria produced methanethiol (*9*), MGL has been characterized from bacteria, including *Clostridiums porogenes* (*10*), *Pseudomonas ovalis* (*11*), *Pseudomonas putida* (*12*), *Aeromonas* sp. (*13*), *Citrobacter intermedius* (*14*), *Brevibacterium linens* (*15*), *Citrobacter freundii* (*16*), *Porphyromonas gingivalis* (*17*), and *Treponema denticola* (*18*), parasitic protozoa such as *Trichomonas vaginalis* (*19*), *Entamoeba histolytica* (*20*), and a model plant *Arabidopsis thaliana* (*21*). MGL activity was also detected from archaeon *Ferroplasma acidarmanus* (*22*), cheese surface bacteria such as *Micrococcus luteus, Arthrobacter* sp., *Corynebacterium glutamicum*, and *Staphylococcus equorum* (*23*). Crystal structures have been reported from *Pseudomonas putida*, (*24-26*), *Citrobacter freundii* (*27*, *28*), *Trichomonas vaginalis* (PDB ID: 1E5F and 1PFF), and *Entamoeba histolytica* (*29*, *30*). In this review, we outline our current understanding of the distribution among organisms, enzymological properties, and the reaction mechanisms of MGL. We then discuss the present status of practical applications exploiting MGL, namely drug development against pathogens and cancers.

ENZYMOLOGICAL PROPERTIES

Basic Reactions, Size, and Cofactor

MGL catalyzes the α, γ-elimination of L-methionine and its derivatives such as L-homocysteine, L-ethionine, and L-selenomethionine (Fig. 2). It also catalyzes the α, β-elimination of L-cysteine and its analogs such as *S*-methyl-L-cysteine (*31*). These reactions yield α-keto acid (2-oxobutyrate and pyruvate), ammonia, and thiols (methanethiol and hydrogen sulfide). It also degrades *O*-substituted serine or homoserine such as *O*-acetyl-L-serine, *O*-acetyl-L-homoserine, and *O*-succinyl-L-homoserine, and release organic acids instead of thiols. This enzyme alternatively catalyzes β- or γ-replacement reactions, where the sulfur or oxygen atom at the β- or γ-position of the substrate is replaced with the thiol. For example, the methy thiol moiety of L-methionine is replaced by ethanethiol to yield ethionine and mechanethiol (*11*). MGL also catalyzes deamination and γ-addition reaction of L-vinylglycine (*31*). MGL consists of 389–441 amino acids, and forms homotetramer. The active MGL tetramer consists of two sets of the catalytic dimers (Fig. 3, panel A; green/yellow and red/blue pairs) that are tightly associated. (*24*, *26*, *27*). The active site is formed at the interface of the two neighboring subunits. Each subunit contains one pyridoxal 5′- phosphate (PLP) as a cofactor (Fig. 3, panel B). MGL is categorized into the γ-family of PLP-dependent enzymes (*32*).

Reaction Mechanisms

Based on the reaction mechanism of PLP γ-family enzymes hitherto known and the enzymological analyzes of *P. putida* MGL wild-type and mutants, it has been proposed that MGL catalyzes elimination reaction in the following order: (1) a Schiff-base linkage between PLP and the lysine residue displaces the binding of the primary amino group of the substrate and

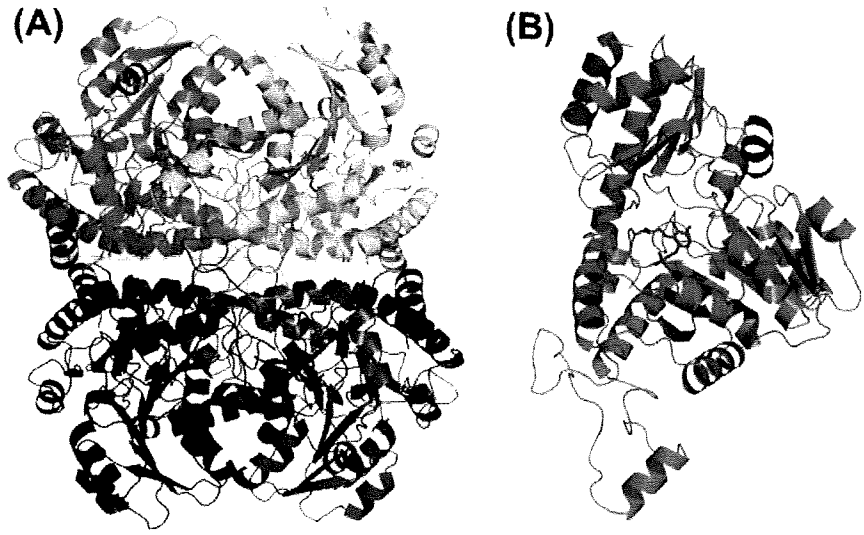

Figure 3. Crystal structure of MGL. (A) The overall structure of *E. histolytica* MGL2. (Harada et al., unpublished). Each subunit consisting the homotetramer is indicated in green, yellow, red, and blue. PLP is indicated in magenta. (B) A single subunit of *E. histolytica* MGL2.

PLP, to form an external aldimine, (2) α- and β-hydrogens of the substrate are shifted to PLP, (3) the phenolic group of the adjacent tyrosine residue attacks the γ-position of the substrate as an acid catalyst, (4) the thiol group is eliminated from the substrate, and (5) α-keto acid and ammonia are released from PLP (*31*, *33*, *34*) (Fig. 4). The mutational studies of *E. histolytica* MGL supported the assumption of an acid catalyst of the tyrosine residue (*35*).

Amino Acid Residues Implicated in Catalysis

Recently, structural analysis of *P. putida* MGL revealed that the six amino acid residues, Tyr59, Arg61, Tyr114, Cys116, Lys240, and Asp241 are located in the vicinity of the substrate binding pocket, close to PLP (*26*). Aside from the amino acid residues conserved among PLP γ-family enzymes (*20*, *24-26*, *36*), a line of evidence indicates that Cys116 of *P. putida* MGL takes part in the unique enzymatic reactions of MGL. This cysteine is not conserved in other PLP γ-family enzymes, and substituted by glycine or proline in cystathionine γ-lyase, cystathionine β-lyase, and cystathionine β-synthase (*26*), and thus was previously suggested to be involved in the recognition and γ-elimination of methionine (*37*). Unlike other MGLs, *B. linens* MGL degrades neither cysteine nor cystathionine, whereas *A. thaliana* MGL degrades cysteine, but hardly cystathionine (*38*). In both *B. linens* and *A. thaliana* MGL, the corresponding cysteine residue was substituted by glycine (*15*, *38*).

The mutational studies of *E. histolytica* and *T. vaginalis* MGL isozymes also demonstrated that the corresponding cysteine residue directly contributes to the substrate specificity. When this cysteine was replaced with glycine or serine, the Km

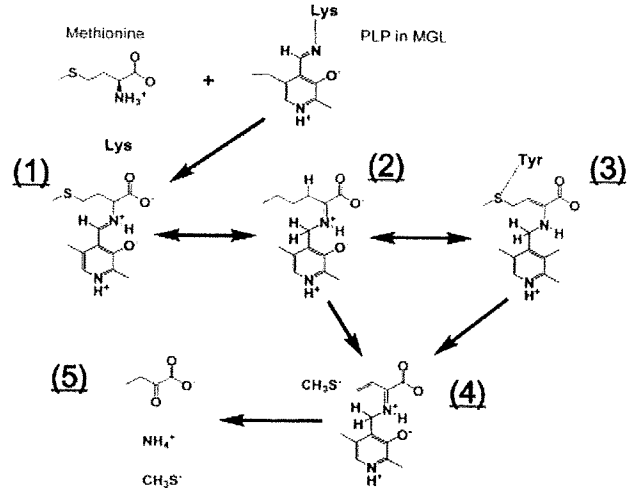

Figure 4. A proposed reaction process of α,γ-elimination of methionine by MGL [modified from (*31*, *33*, *34*)]. Substrates, intermediates, and products are shown in red, while PLP is shown in black. Structures (*1*) to (*5*) correspond to the reaction intermediates explained in the text.

values of one isozyme for methionine and cysteine were drastically changed, while those of the other isotype remained unaltered (*35*, *39*).

In *P. putida* MGL, chemical modification with 2-nitrothiocyanobenzoic acid and labeling with a PLP analog, N-(bromoacetyl)pyridoxamine phosphate, suggested the catalytic importance of Cys116 (*40*, *41*). The substitution of this cysteine to

Table 1
Summary of the fates and roles of the degradation products generated by MGL in various organisms

Products	Final products	Physiological roles	Organisms	Reference
2-Oxobutyrate	Propionate	ATP generation[a]	Anaerobic bacteria	42
			Parasitic protozoa	43 (See Fig. 5)
	Isoleucine	Isoleucine biosynthesis[b]	Plant (*A. thaliana*)	21
	2,3-pentanedione	Unknown	Cheese ripening bacteria	44
Methanethiol	Methanethiol	Host invasion[b] (pathogenicity)	Periodontal bacteria	17
	Methanethiol Dimethyl disulfide Dimethyl trisulfide Thioesters	Unknown (Odor formation of cheese)	Cheese ripening bacteria	44, 45
	S-methyl-cysteine	Sulfur storage[a]	Plant (*A. thaliana*)	21
	Methanethiol Dimethyl sulfide Dimethyl disulfide Dimethyl trisulfide	Defense against herbivorous insects[c]	Plant (guava)	46

[a]Roles only suggested.
[b]Roles experimentally demonstrated.
[c]The presence of *MGL* gene is confirmed only in *A. thaliana*, but not in guava. The volatile thiols may be produce by enzymes other than MGL in guava leaves.

histidine caused a drastic increase or decrease in the activity of MGL toward cysteine or methionine, respectively; their catalytic efficiency (kcat/Km) for cysteine increased by 16.2 fold, while that for methionine decreased by 552 fold, mainly due to the reduction in kcat (*37*). Similar changes in the activity were also observed for methionine and cysteine analogs (*37*).

The crystal structure revealed that the cysteine residue is located in the proximity of a tyrosine residue (*24*), which attacks the γ-position of the substrate (*33*) [see Fig. 4, intermediate (*3*)]. However, direct interaction between the cysteine residue of MGL and methionine, as a substrate, was not observed. Thus, the structures of MGL/methionine intermediates at various reaction stages should be resolved to elucidate how the cysteine residue is involved in γ-elimination of methionine.

PHYSIOLOGICAL FUNCTIONS

The physiological roles of MGL have been either directly demonstrated or indirectly suggested in several organisms (summarized in Table 1).

Association with Anaerobic Metabolism

Anaerobic bacteria and parasitic protozoa that possess MGL, rely on glycolysis and amino acid degradation for energy generation (*42*, *46*). In those anaerobic organisms, for example, anaerobic amitochondrial parasites, pyruvate is converted to acetate via acetyl-CoA (Fig. 5). The conversion proceeds in two sequential reactions catalyzed by pyruvate:ferredoxin oxidoreductase (PFOR, EC. 1. 2. 7. 1) and acetate-CoA ligase (ADP-forming) (EC. 6. 2. 1. 13). In this process, one ATP is generated from one pyruvate. As 2-oxobutyrate, generated from

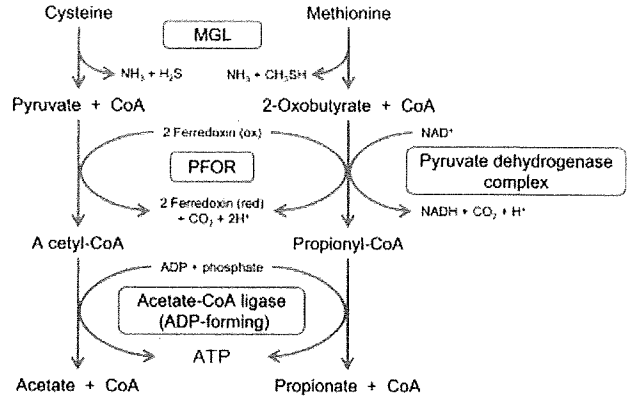

Figure 5. A proposed reaction scheme of energy generation from 2-oxobutyrate. 2-Oxobutyrate, generated from methionine by MGL, serves as a substrate for PFOR or pyruvate dehydrogenase complex, which leads to the ATP generation. "ox" and "red" are the oxidized and reduced form of ferredoxin, respectively. [Color figure can be viewed in the online issue, which is available at www.interscience.wiley.com.]

methionine by MGL, is condensed with CoA to form propionyl-CoA, which is in turn decomposed by acetate-CoA ligase (ADP-forming) with a concomitant ATP generation, the process might contribute to energy metabolism.

The Bioenergetic Roles of MGL in Bacteria

In *P. putida*, MGL gene is transcribed as a part of an operon containing 2-oxobutyrate decarboxylase (*47*, *48*), both of which

appear to be coordinately regulated (Inoue and Inagaki, unpublished). Although 2-oxobutyrate decarboxylase is homologous to homodimeric-type E1 component of pyruvate dehydrogenase complex (*47, 48*), its catalytic efficiency (kcat/Km) is 29-fold higher for 2-oxobutyrate than toward pyruvate (*47, 48*). E2 component, which produces acetyl-CoA by transferring the acetyl group to CoA, is also annotated in the genome database (http://www.pseudomonas.com/). Although E3 (dihydrolipoyl dehydrogenase) appears to be absent in the genome, it is conceivable that *P. putida* is capable of producing ATP via this pathway.

The Other Roles of MGL in Bacteria

MGL has been implicated in the pathogenicity of periodontal bacterium, *P. gingivalis* using a mouse model (*17*). It was shown that only 7.7% of mice infected with wild-type *P. gingivalis* survived, whereas 36% of mice infected with MGL-deficient mutant survived, at 4 days after subcutaneous injection of bacteria. No direct evidence for the involvement of MGL in the pathogenesis in other bacteria is available.

In the cheese ripening bacterium *B. linens*, methanethiol and 2-oxobutyrate are produced by MGL (*44*). Methanethiol is converted to dimethyl disulfide, dimethyl trisulfide, and thioesters, and 2-oxobutyrate is condensed with active acetaldehyde derived from pyruvate, and metabolized to 2,3-pentanedione (acetyl propionyl) (*44*). This condensation reaction is catalyzed by acetolactate synthase (*44, 45*). Under the methionine-rich conditions, genes encoding MGL, acetolactate synthase (see below), and α-keto acid dehydrogenases are up-regulated (*45*). Thus, methionine degradation is tightly linked with carbohydrate metabolism in this and related bacteria. The physiological importance of 2,3-pentanedione has not been demonstrated.

The Roles of MGL in Plants

In the model plant *A. thaliana*, MGL is expressed in various tissues. The regulation of its expression in seeds is peculiar. It was shown that while MGL mRNA was highly accumulated but not translated in dry seeds, the protein was highly expressed in imbibed seeds (*21*). This unique regulation of MGL expression suggests that immediate production of MGL protein is essential in the early germination process. These data suggest that while MGL is implicated in methionine homeostasis in various tissues, it plays an important role in the resumption process (*21*).

Methanethiol and 2-oxobutyrate, the degradation products of methionine by MGL, are used for the synthesis of *S*-methyl-L-cysteine and isoleucine, respectively. *S*-methyl-L-cysteine is a potential storage molecule of sulfur, similar to the metabolites of methionine cycle such as *S*-adenosyl-L-methionine, and *S*-methyl-L-methionine (*21*). Functional analysis of a MGL-deficient *A. thaliana* mutant revealed that MGL is involved in the alternative reverse-transsulfuration pathway, in which methionine is metabolized to cysteine, not via cystathionine (*38*). Methanethiol was potentially an intermediate of this pathway, although a detailed process of flux was elusive (*38*). However, the methionine degradation by *A. thaliana* MGL was three orders of magnitude lower than that by MGL from other organisms, for example, the kcat/Km values of *A. thaliana* MGL was 0.0022 S^{-1} mM^{-1}, whereas those of *P. putida* and *E. histolytica* were 54 and 2.99, respectively (*33, 35, 38*). Therefore, the possibility that *A. thaliana* MGL predominantly catalyzes a replacement reaction, rather than degradation, was not excluded. More detailed enzymological characterization including identification of an acceptor of methanethiol is necessary to fully characterize the pathway.

Recently, it has been reported that wounded leaves of guava produce the volatile sulfur compounds including methanethiol as defense molecules against herbivorous insects (*46*). Although MGL has not yet been demonstrated in guava, and it remains unknown if this mechanism exists ubiquitously in plants, the productions of sulfur compounds with anti-insect activity might be the major physiological function of MGL in plants.

Function and Lateral Gene Transfer-Dependent Acquisition of MGL Isotypes in Parasitic Protozoa

Both of the MGL-containing parasitic protists *E. histolytica* and *T. vaginalis* possess two isozymes of MGL with high mutual identity (69%) and distinct substrate specificities (*20, 35, 39*). In *E. histolytica*, one isozyme (i.e., *Eh*MGL1) degrades methionine more efficiently than homocysteine, while the other (*Eh*MGL2) prefers homocysteine to methionine (*35, 39*). In contrast, one isozyme of *T. vaginalis* MGL (*Tv*MGL1) seems predominantly to degrades methionine, homocysteine, and cysteine compared to the other (*Tv*MGL2) (*35, 39*). Considering that MGL isozymes have been found only in the parasitic protozoa, the multiplicity of MGLs might be related to the parasitic style or pathogenesis.

It was proposed that MGL in extant protozoan parasites was acquired by lateral gene transfer, together with the enzymes related to anaerobic energy metabolism (*20, 49*). Interestingly, the origin of MGL in the two parasitic protozoa was not identical (*20*). *E. histolytica* MGLs show a monophylic relationship with MGL from archaea, while *T. vaginalis* MGLs have strong affinity to MGLs of bacterial origin, suggesting that lateral gene transfer of MGL to the two protists occurred independently.

Other Undiscovered Roles

Since the substrate specificity of MGL varies among organisms, the physiological role of MGL, other than the maintenance of SAA homeostasis, can be also organism specific. Although MGL catalyzes homocysteine *in vitro*, it remains questionable whether it is responsible for the degradation of homocysteine *in vivo* because the cellular concentrations of homocysteine are predicted to be extremely low [e.g., the concentration in human plasma is less than 10 μM (*50*)] compared to the Km values of MGLs.

The physiological role of MGL has not been investigated in archaea. In an acidophilic iron-oxidizing euryarchaeon

Ferroplasma acidarmanus, methanethiol has been demonstrated, while its draft genome apparently lacks a gene encoding MGL or similar enzymes (The UCSC Archaeal Genome Browser at http://archaea.ucsc.edu/). Thus, it is feasible that in *F. acidarmanus*, methionine is degraded in two step reactions consisting an amino transfer, which yields 4-methylthio-2-oxobutyric acid, and chemical decompose into 2-oxobutyrate, as proposed for methionine catabolic pathway in yeast *Geotrichum candidum* (*44*).

DRUG DEVELOPMENT EXPLOITING MGL

Mechanisms of Trifluoromethionine (TFM) Targeting MGL in Pathogens

The emergence of drug resistance and adverse effects of available chemotherapeutics always necessitate discovery and development of new drugs targeting unexplored enzymes and pathways. The unique catalytic reaction of MGL and its limited distribution in pathogens, but not in human, makes the enzyme a promising target to design novel chemotherapeutic agents against amebiasis, trichomoniasis, and gum diseases (*51, 52*). Trifluoromethionine (*S*-trifluoromethyl-L-homocysteine, TFM), a fluorinated methionine in which three hydrogens of the methyl group are replaced by fluorines, was designed in the wake of successful use of metabolite analog such as 6-mercaptopurine (*53*).

Microbicidal mechanisms of TFM have been proposed. One of the products of TFM degraded by MGL, trifluoromethanethiol (trifluoromethylmercaptan), is converted non-enzymatically to carbonothionic difluoride, subsequently crosslinks the primary amino group of proteins, and causes toxicity (*35, 54*). We reported that TFM was preferentially degraded by one of the two *E. histolytica* isozymes, *Eh*MGL2, and less efficiently by *Eh*MGL1 (*35*). Site-directed mutagenesis of *Eh*MGL1 and *Eh*MGL2 indicated that mechanisms of degradation differed between TFM and physiological substrates. Interestingly, the MGL mutants where the arginine residue that plays a critical role in the fixation of PLP was replaced by alanine, still retained activities against TFM, while they lost activities toward physiological substrates. These results imply that the degradation of TFM probably proceeds without interaction with other amino acid residues, possibly due to the electronegativity of the trifluoromethyl group of TFM (*35*).

Antimicrobial Spectrum of TFM

TFM is highly toxic to various anaerobic microorganisms. The minimal inhibitory concentrations against *Mycobacterium smegmatis, Mycobacterium phlei,* and *Candida lipolytica* were estimated to be 24.6–49.3 μM (*55*). The growth of periodontal bacteria *P. gingivalis* and *F. nucleatum* was retarded by 0.1 mM TFM and completely inhibited by 1 mM (*56*). *T. vaginalis* was killed at 24.6 μM within 24 h *in vitro* (*57*). The IC_{50} value of TFM against the *E. histolytica in vitro* culture was estimated to be 7.3 μM, comparable to metronidazole, the commonly used drug (*58*).

The efficacy of TFM has also been tested *in vivo*. The single intravenous administration of 40 mg/kg of TFM to mice infected by the subcutaneous inoculation of *T. vaginalis* 2 h before the TFM treatment caused the lesion to be almost cured (five of six TFM-treated mice produced no lesion) (*57*). Survival rate of mice that received subcutaneous inoculation of *P. gingivalis* 3 days prior increased by 3.2-fold when coinjected with 4 μmol of TFM (*56*). A single subcutaneous and oral administration of TFM (1.02 and 2.54 mg/ kg each) after 24 h of intrahepatic inoculation of *E. histolytica* trophozoites also cured amoebic liver abscesses in hamsters (*58*).

Selectivity of TFM

TFM is a prodrug which shows toxicity only after degradation by MGL. In fact, TFM showed no growth retardation or killing to MGL-deficient *P. gingivalis* (*17*). The growth inhibition of *T. vaginalis* by TFM was abolished by propargylglycine, a suicide substrate of MGL (*57*). Growth of *Giardia lamblia*, the parasite of duodenum and small intestine that causes watery diarrhea, and shares anaerobic energy metabolism with *E. histolytica* and *T. vaginalis*, but lacks MGL, was affected by only very high concentration of TFM (493 μM) (*57*). The growth of *E. coli* expressing *T. vaginalis* MGL was inhibited by TFM in a dose-dependent manner (*57*), while wild type *E. coli* was not affected by TFM (*56*). Although *E. coli* has cystathionine gamma-lyase and cystathionine gamma-synthase, both of which are structurally similar to MGL (*32*), TFM does not affect growth of *E. coli*.

Although TFM is structurally very similar to methionine, both utilization of TFM via the methionine cycle, initiated by methionine adenosyltransferase, and incorporation into proteins are extremely poor (*59, 60*). Furthermore, TFM did not affect the mammalian cystathionine gamma-lyase (*54*). In addition, TFM has little cytotoxic effect on mammalian cells. TFM at 493μM did not inhibit the growth of mouse myeloma cells (*57*) and CHO cells [the IC_{50} against CHO cells was 709 μM (*58*)]. These data support that cytotoxic effects of TFM is specific to MGL and reinforce the selectivity of TFM against pathogens harboring MGL.

Derivatization of TFM to Improve Efficacy

To improve the cytotoxicity of TFM, we synthesized various amide derivatives of TFM. Several TFM amide derivatives showed higher cytotoxic effects against *E. histolytica in vitro* compared to TFM and metronidazole (*58*). Kinetic studies with recombinant enzymes showed that the TFM amide derivatives were degraded by MGL, less efficiently compared to TFM. TFM amide derivatives appeared to be first hydrolyzed by cysteine proteases and metalloproteases in amebic cell lysate, and subsequently degraded by the α, γ-elimination by MGL (*58*).

These results should help us to further improve the efficiency of TFM.

Novel MGL Inhibitor

Recently, it has been shown that myrsinoic acid B, a terpenobenzoic acid, extracted from *the leaves of Myrisine Seguinii* Lév, has an inhibitory effect on MGL activity (*61*). It is thus the first natural MGL inhibitor reported. Myrsinoic acid B was also reported to possess anti-inflammatory activity against edema of mouse ear induced by skin tumor promoter (*62*). Myrsinoic acid B inhibited the production of 2-oxobutyrate in the crude extract of periodontal bacteria, *F. nucleatum, P. gingivalis,* and *T. denticola*. The IC_{50} values of myrsinoic acid B against these bacteria were estimated to be 0.389 μM, 82.4 μM, or 30.3 μM, respectively. Thus, these MGL inhibitors would be potentially useful for the prevention of oral malodor and periodontal diseases. For practical applications, it is important to show the specificity of myrsinoic acid B, and to exclude a possibility that it affects mammalian γ-family members of PLP-enzymes.

The physiological role of myrsinoic acid B in plants has not been demonstrated, similar to many other secondary metabolites. Assumed that myrsinoic acid B inhibits the endogenous MGL in *Myrisine Seguinii* Lév, it may control isoleucine synthesis by repressing methionine degradation. The other possibility is that myrsinoic acid B negatively regulates the release of methanethiol to allow inhabitation or parasitization by insects. It may be worth comparing the concentration of myrsinoic acid B and the MGL activity between intact and wounded leaves.

UTILIZATION OF MGL FOR THE TREATMENT OF CANCERS

Rationale of MGL for Cancer Treatment

Many cancer cells have an absolute requirement for plasma methionine, whereas normal cells are relatively resistant to the restriction of exogenous methionine (*63*). Methionine depletion has a broad spectrum of antitumor activities (*64*). Under methionine depletion, cancer cells were arrested in the late S-G2 phase due to the pleiotropic effects and underwent apoptosis. Thus, therapeutic exploitation of *P. putida* MGL to deplete plasma methionine has been extensively investigated (*64*). Growth of various tumors such as Lewis lung carcinoma (*65*), human colon cancer lines (*66*), glioblastoma (*67*), and neuroblastoma (*68*) was arrested by MGL. MGL in combination with anticancer drugs such as cisplatin, 5-fluorouracil, nitrosourea, and vincristine displayed synergistic antitumor effects on rodent and human tumors in mouse models (*65–68*). It was also reported that MGL introduced by adenovirus vector inhibited the growth of tumors *in vitro*. MGL, when combined with selenomethionine, a suicide prodrug substrate of MGL, inhibited tumor growth in rodents and prolonged their survivals (*69*). Methaneselenol produced by decomposition of selenomethionine, was oxidized to methylseleninic acid, which in turn oxidized protein sulfhydryls and generated reactive oxygen species, and was then reduced back to selenol by glutathione (*70*). In addition to the synergistic effects noted above, the advantage of anticancer therapy using MGL is its wide range of target tumors, including those resistant to the conventional chemotherapeutics and radiation. Taken together, MGL treatment will provide a novel paradigm for cancer therapy.

Modifications of MGL to Reduce its Side Effects

It was reported that administration of MGL caused anaphylactic shock in macaque monkeys (*71*). To overcome this problem, polyethylene glycol-conjugated MGL (PEG-MGL) was constructed. PEG-MGL reduced immunogenicity; the IgG titers decreased by 10 to 10,000-fold, depending on the binding rate of PEG and MGL, compared to naked MGL. The half life and depletion time of MGL in the mouse plasma was improved by PEG conjugation. The enzymatic activity of PEG-MGL was detected for 72 h, while that of unconjugated MGL was undetectable after 24 h, and the half life of PEG-MGL increased by ~20 times (38 h), compared to unconjugated MGL (2 h) (*72*). Simultaneous coadministration of pyridoxal 5′-phosphate and oleic acid, or dithiothreitol treatment also strengthened effectiveness of PEG-MGL in the rodent model (*72, 73*).

OTHER APPLICATIONS OF MGL

Elevated blood and serum homocysteine is known as a notorious risk factor for cardio-vascular diseases, dementia, and Alzheimer's disease (*74*). It was reported that the administration of the combination of vitamins (folic acid, vitamins B_6, and B_{12}) decreased homocysteine concentrations, but did not significantly reduce the risk of death from cardio-vascular diseases (*75–77*). Thus, therapeutic interventions by directly lowering homocysteine by the administration of MGL may be worth attempting.

The unique enzymological properties of MGL was applied to clinical examination of homocysteine, cysteine, and PLP (*78-80*). These examination methods utilizing MGL with sufficient sensitivities are suitable for mass screening and, thus, can be an economical alternate of the expensive HPLC-dependent method.

PERSPECTIVES

Although MGL has been explored to be an ideal drug target against microbial infections and also for the treatment of cancers, its reaction mechanism and physiological functions remain to be fully elucidated. Recently structural analyzes of wild type and mutant MGLs have been reported (*26, 35, 37*), which disclose the substrate recognition and reaction mechanisms. In addition, the tertiary structures of MGLs were resolved (*24–26, 28–30*) PDB ID: 1E5F and 1PFF), including the complex with inhibitors (PDB ID, 1E5E; Harada, et al., unpublished). To further elucidate the reaction mechanisms, the tertiary structures of various stages of the MGL-substrate/prodrug/inhibitor complex need to be resolved. These data should lead to a further fine

adjustment of anti-infective agents targeting MGL and anti-cancer drugs exploiting MGL.

The acquisition and conservation of MGL in a limited lineage of bacteria and archaea remain one of the major unsolved issues. Manukhov et al. reported that the *C. freundii* has a MGL gene while its vestigial gene was found in the other bacteria in Enterobacteriaceae family, such as *Salmonella enterica* serovar Typhimurium, *Shigella flexneri*, *E. coli*, and *C. rodentium* (*81*). These bacteria appear to have acquired MGL by lateral gene transfer from a common ancestor, and the latter have lost the function of MGL. To compensate the secondary loss of MGL, these bacteria might utilize an alternative pathway, as shown in yeast *G. candidum*. In this pathway, methionine degradation is initiated by transamidation, which forms 4-methylthio-2-oxobutyrate, followed by a cleavage to yield 2-oxobutyrate and methanethiol by chemical process (*44*). The comparative metabolomics and fluxomics between the bacteria possessing or lacking MGL should help our understanding its biological importance of MGLs.

As far as the genome is available, only the unicellular parasitic protozoa possess two MGL isozymes with distinct substrate specificities. This unique redundancy might be related to the parasitic life styles, for example, the acquisition of nutrients from the human host and the complex life cycle. Reverse genetic approaches (*82*, *83*) or specific inhibitors, in combination with "omics" approaches including metabolomics/transcriptmics should delineate individual roles of the isotypes.

ACKNOWLEDGEMENTS

The authors thank Dr. Shigeharu Harada and Mr. Tsuyoshi Karaki, Department of Applied Biology, Kyoto Institute of Technology, for kindly permitting them to use the images of crystal structures of *E. histolytica* MGL. This work was supported by a Grant-in-Aid for Scientific Research from the Ministry of Education, Culture, Sports, Science and Technology of Japan to D.S. (20590429) and T.N. (18GS0314, 18050006, 18073001), a grant for research on emerging and re-emerging infectious diseases from the Ministry of Health, Labor and Welfare of Japan (H20-Shinkosaiko-016), and a grant for research to promote the development of anti-AIDS pharmaceuticals from the Japan Health Sciences Foundation to T.N.

REFERENCES

1. Nozaki, T., Ali, V., and Tokoro, M. (2005) Sulfur-containing amino acid metabolism in parasitic protozoa. *Adv. Parasitol.* **60**, 1–99.
2. Stipanuk, M. H. (2004) Sulfur amino acid metabolism: pathways for production and removal of homocysteine and cysteine. *Annu. Rev. Nutr.* **24**, 539–577.
3. De Bree, A., Verschuren, W. M., Kromhout, D., Kluijtmans, L. A., and Blom, H. J. (2002) Homocysteine determinants and the evidence to what extent homocysteine determines the risk of coronary heart disease. *Pharmacol. Rev.* **54**, 599–618.
4. Wald, D. S., Law, M., and Morris, J. K. (2002) Homocysteine and cardiovascular disease: evidence on causality from a meta-analysis. *BMJ* **325**, 1202–1206.
5. Morris, M. S. (2003) Homocysteine and Alzheimer's disease. *Lancet. Neurol.* **2**, 425–428.
6. Joseph, C. A. and Maroney, M. J. (2007) Cysteine dioxygenase: structure and mechanism. *Chem. Commun. (Camb.)* 3338–3349.
7. Uren, J. R. (1987) Cystathionine beta-lyase from *Escherichia coli*. *Methods. Enzymol.* **143**, 483–486.
8. Ravanel, S., Job, D., and Douce, R. (1996) Purification and properties of cystathionine beta-lyase from *Arabidopsis thaliana* overexpressed in *Escherichia coli*. *Biochem. J.* **320**, 383–392.
9. Onitake, J. (1938) On the formation of methyl mercaptan from L-cystine and L-methionine by bacteria. *J. Osaka Med. Assoc.* **37**, 263–270.
10. Kreis, W. and Hession, C. (1973) Isolation and purification of L-methionine-alpha-deamino-gamma-mercaptomethane-lyase (L-methioninase) from *Clostridium sporogenes*. *Cancer. Res.* **33**, 1862–1865.
11. Tanaka, H., Esaki, N., and Soda, K. (1977) Properties of L-methionine gamma-lyase from *Pseudomonas ovalis*. *Biochemistry* **16**, 100–106.
12. Nakayama, T., Esaki, N., Sugie, K., Beresov, T. T., Tanaka, H., and Soda, K. (1984) Purification of bacterial L-methionine gamma-lyase. *Anal. Biochem.* **138**, 421–424.
13. Nakayama, T., Esaki, N., Lee, W.-J., Tanaka, I., Tanaka, H., and Soda, K. (1984) Purification and properties of L-methionine γ-lyase from *Aeromonas* sp. *Agric. Biol. Chem.* **48**, 2367–2369.
14. Faleev, N. G., Troitskaya, M. V., Paskonova, E. A., Saporovskaya, M. B., and Belikov, V. M. (1996) L-methionine-γ-lyase in *Citrobacter intermedius* cells: stereochemical requirements with respect to the thiol structure. *Enzyme. Microb. Technol.* **19**, 590–593.
15. Dias, B. and Weimer, B. (1998) Purification and characterization of L-methionine gamma-lyase from *Brevibacterium linens* BL2. *Appl. Environ. Microbiol.* **64**, 3327–3331.
16. Manukhov, I. V., Mamaeva, D. V., Morozova, E. A., Rastorguev, S. M., Faleev, N. G., Demidkina, T. V., and Zavilgelsky, G. B. (2006) L-methionine gamma-lyase from *Citrobacter freundii*: cloning of the gene and kinetic parameters of the enzyme. *Biochemistry (Mosc).* **71**, 361–369.
17. Yoshimura, M., Nakano, Y., Yamashita, Y., Oho, T., Saito, T., and Koga, T. (2000) Formation of methyl mercaptan from L-methionine by *Porphyromonas gingivalis*. *Infect. Immun.* **68**, 6912–6916.
18. Fukamachi, H., Nakano, Y., Okano, S., Shibata, Y., Abiko, Y., and Yamashita, Y. (2005) High production of methyl mercaptan by L-methionine-alpha-deamino-gamma-mercaptomethane lyase from *Treponema denticola*. *Biochem. Biophys. Res. Commun.* **331**, 127–131.
19. Lockwood, B. C. and Coombs, G. H. (1991) Purification and characterization of methionine gamma-lyase from *Trichomonas vaginalis*. *Biochem. J.* **279**, 675–682.
20. Tokoro, M., Asai, T., Kobayashi, S., Takeuchi, T., and Nozaki, T. (2003) Identification and characterization of two isoenzymes of methionine gamma-lyase from *Entamoeba histolytica*: a key enzyme of sulfur-amino acid degradation in an anaerobic parasitic protist that lacks forward and reverse trans-sulfuration pathways. *J. Biol. Chem.* **278**, 42717–42727.
21. Rébeillé, F., Jabrin, S., Bligny, R., Loizeau, K., Gambonnet, B., Van Wilder, V., Douce, R., and Ravanel, S. (2006) Methionine catabolism in *Arabidopsis cells* is initiated by a gamma-cleavage process and leads to *S*-methylcysteine and isoleucine syntheses. *Proc. Natl. Acad. Sci. USA* **103**, 15687–15692.
22. Baumler, D. J., Hung, K. F., Jeong, K. C., and Kaspar, C. W. (2007) Production of methanethiol and volatile sulfur compounds by the archaeon "Ferroplasma acidarmanus." *Extremophiles* **11**, 841–851.
23. Bonnarme, P., Psoni, L., and Spinnler, H. E. (2000) Diversity of L-methionine catabolism pathways in cheese-ripening bacteria. *Appl. Environ. Microbiol.* **66**, 5514–5517.
24. Motoshima, H., Inagaki, K., Kumasaka, T., Furuichi, M., Inoue, H., Tamura, T., Esaki, N., Soda, K., Tanaka, N., Yamamoto, M., and Tanaka, H. (2000) Crystal structure of the pyridoxal 5′-phosphate

dependent L-methionine gamma-lyase from *Pseudomonas putida*. *J. Biochem. (Tokyo)* **128**, 349–354.

25. Sridhar, V., Xu, M., Han, Q., Sun, X., Tan, Y., Hoffman, R. M., and Prasad, G. S. (2000) Crystallization and preliminary crystallographic characterization of recombinant L-methionine-alpha-deamino-gamma-mercaptomethane lyase (methioninase). *Acta. Crystallogr. D. Biol. Crystallogr.* **56**, 1665–1667.
26. Kudou, D., Misaki, S., Yamashita, M., Tamura, T., Takakura, T., Yoshioka, T., Yagi, S., Hoffman, R. M., Takimoto, A., Esaki, N., and Inagaki, K. (2007) Structure of the antitumour enzyme L-methionine gamma-lyase from *Pseudomonas putida* at 1.8 Å resolution. *J. Biochem. (Tokyo)* **141**, 535–544.
27. Mamaeva, D. V., Morozova, E. A., Nikulin, A. D., Revtovich, S. V., Nikonov, S. V., Garber, M. B., and Demidkina, T. V. (2005) Structure of *Citrobacter freundii* L-methionine gamma-lyase. *Acta. Crystallogr. Sect. F Struct. Biol. Cryst. Commun.* **61**, 546–549.
28. Nikulin, A., Revtovich, S., Morozova, E., Nevskaya, N., Nikonov, S., Garber, M., and Demidkina, T. (2008) High-resolution structure of methionine gamma-lyase from *Citrobacter freundii*. *Acta. Crystallogr. D. Biol. Crystallogr.* **64**, 211–218.
29. Sato, D., Yamagata, W., Kamei, K., Nozaki, T., and Harada, S. (2006) Expression, purification and crystallization of L-methionine gamma-lyase 2 from *Entamoeba histolytica*. *Acta. Crystallogr. Sect. F Struct. Biol. Cryst. Commun.* **62**, 1034–1036.
30. Sato, D., Karaki, T., Shimizu, A., Kamei, K., Harada, S., and Nozaki, T. (2008) Crystallization and preliminary x-ray analysis of L-methionine gamma-lyase 1 from *Entamoeba histolytica*. *Acta. Crystallogr. Sect. F Struct. Biol. Cryst. Commun.* **64**, 697–699.
31. Tanaka, H., Esaki, N., and Soda, K. (1985) A versatile bacterial enzyme: L-methionine γ-lyase. *Enzyme. Microb. Technol.* **7**, 530–537.
32. Alexander, F. W., Sandmeier, E., Mehta, P. K., and Christen, P. (1994) Evolutionary relationships among pyridoxal-5′-phosphate-dependent enzymes. Regio-specific alpha, beta and gamma families. *Eur. J. Biochem.* **219**, 953–960.
33. Inoue, H., Inagaki, K., Adachi, N., Tamura, T., Esaki, N., Soda, K., and Tanaka, H. (2000) Role of tyrosine 114 of L-methionine gamma-lyase from *Pseudomonas putida*. *Biosci. Biotechnol. Biochem.* **64**, 2336–2343.
34. Toney, M. D. (2005) Reaction specificity in pyridoxal phosphate enzymes. *Arch. Biochem. Biophys.* **433**, 279–287.
35. Sato, D., Yamagata, W., Harada, S., and Nozaki, T. (2008) Kinetic characterization of methionine gamma-lyases from the enteric protozoan parasite *Entamoeba histolytica* against physiological substrates and trifluoromethionine, a promising lead compound against amoebiasis. *FEBS. J.* **275**, 548–560.
36. Inoue, H., Inagaki, K., Sugimoto, M., Esaki, N., Soda, K., and Tanaka, H. (1995) Structural analysis of the L-methionine gamma-lyase gene from *Pseudomonas putida*. *J. Biochem. (Tokyo).* **117**, 1120–1125.
37. Kudou, D., Misaki, S., Yamashita, M., Tamura, T., Esaki, N., and Inagaki, K. (2008) The role of cysteine 116 in the active site of the antitumor enzyme L-methionine gamma-lyase from *Pseudomonas putida*. *Biosci. Biotechnol. Biochem.* **72**, 1722–1730.
38. Goyer, A., Collakova, E., Shachar-Hill, Y., and Hanson, A. D. (2007) Functional characterization of a methionine γ-Lyase in *Arabidopsis* and its implication in an alternative to the reverse trans-sulfuration pathway. *Plant. Cell. Physiol.* **48**, 232–242.
39. Mckie, A. E., Edlind, T., Walker, J., Mottram, J. C., and Coombs, G. H. (1998) The primitive protozoon *Trichomonas vaginalis* contains two methionine gamma-lyase genes that encode members of the gamma-family of pyridoxal 5′-phosphate-dependent enzymes. *J. Biol. Chem.* **273**, 5549–5556.
40. Nakayama, T., Esaki, N., Tanaka, H., and Soda, K. (1988) Specific labeling of the essential cysteine residue of L-methionine gamma-lyase with a cofactor analog, *N*-(bromoacetyl)pyridoxamine phosphate. *Biochemistry* **27**, 1587–1591.
41. Nakayama, T., Esaki, N., Tanaka, H., and Soda, K. (1988) Chemical modification of cyseine residues of L-methionine γ-lyase. *Agric. Biol. Chem.* **52**, 177–183.
42. Ragsdale, S. W. (2003) Pyruvate ferredoxin oxidoreductase and its radical intermediate. *Chem. Rev.* **103**, 2333–2346.
43. Müller, M. Coombs, G. H., Vickerman, K., Sleigh, M. A. and, Warren, A., eds. (1998) *Enzymes and Compartmentation of Core Energy Metabolism of Anaerobic Protists—A Special Case in Eukaryotic Evolution?* In *Evolutionary relationships among protozoa.* (Coombs, G.H., Vickerman, K., Sleigh, M.A., Warren, A., ed) pp. 109–131, Kluwer Academic Publishers, London.
44. Arfi, K., Landaud, S., and Bonnarme, P. (2006) Evidence for distinct L-methionine catabolic pathways in the yeast *Geotrichum candidum* and the bacterium *Brevibacterium linens*. *Appl. Environ. Microbiol.* **72**, 2155–2162.
45. Cholet, O., Hénaut, A., and Bonnarme, P. (2007) Transcriptional analysis of L-methionine catabolism in *Brevibacterium linens* ATCC9175. *Appl. Microbiol. Biotechnol.* **74**, 1320–1332.
46. Rouseff, R. L., Onagbola, E. O., Smoot, J. M., and Stelinski, L. L. (2008) Sulfur volatiles in guava (*Psidium guajava* L.) leaves: possible defense mechanism. *J. Agric. Food. Chem.* **56**, 8905–8910.
47. Inoue, H., Inagaki, K., Eriguchi, S. I., Tamura, T., Esaki, N., Soda, K., and Tanaka, H. (1997) Molecular characterization of the *mde* operon involved in L-methionine catabolism of *Pseudomonas putida*. *J. Bacteriol.* **179**, 3956–3962.
48. Inoue, H., Nishito, A., Eriguchi, S. I., Tamura, T., Inagaki, K., and Tanaka, H. (2003) Purification and substrate characterization of α-ketobutyrate decarboxylase from *Pseudomonas putida*. *J. Mol. Catal., B Enzym.* **23**, 265–271.
49. Rosenthal, B., Mai, Z., Caplivski, D., Ghosh, S., De La Vega, H., Graf, T., and Samuelson, J. (1997) Evidence for the bacterial origin of genes encoding fermentation enzymes of the amitochondriate protozoan parasite *Entamoeba histolytica*. *J. Bacteriol.* **179**, 3736–3745.
50. Mudd, S. H., Finkelstein, J. D., Refsum, H., Ueland, P. M., Malinow, M. R., Lentz, S. R., Jacobsen, D. W., Brattstrom, L., Wilcken, B., Wilcken, D. E., Blom, H. J., Stabler, S. P., Allen, R. H., Selhub, J., and Rosenberg, I. H. (2000) Homocysteine and its disulfide derivatives: a suggested consensus terminology. *Arterioscler. Thromb. Vasc. Biol.* **20**, 1704–1706.
51. Ali, V. and Nozaki, T. (2007) Current therapeutics, their problems, and sulfur-containing-amino-acid metabolism as a novel target against infections by "amitochondriate" protozoan parasites. *Clin. Microbiol. Rev.* **20**, 164–187.
52. Nakano, Y., Yoshimura, M., and Koga, T. (2002) Methyl mercaptan production by periodontal bacteria. *Int. Dent. J.* **52**, 217–220.
53. Dannley, R. L. and Taborsky, R. G. (1957) Synthesis of DL-*S*-trifluoromethylhomocysteine (trifluoromethylmethionine). *J. Org. Chem.* **22**, 1275–1276.
54. Alston, T. A. and Bright, H. J. (1983) Conversion of trifluoromethionine to a cross-linking agent by gamma-cystathionase. *Biochem. Pharmacol.* **32**, 947–950.
55. Zygmunt, W. A. and Tavormina, P. A. (1966) DL-*S*-Trifluoromethylhomocysteine, a novel inhibitor of microbial growth. *Can. J. Microbiol.* **12**, 143–148.
56. Yoshimura, M., Nakano, Y., and Koga, T. (2002) L-Methionine-gamma-lyase, as a target to inhibit malodorous bacterial growth by trifluoromethionine. *Biochem. Biophys. Res. Commun.* **292**, 964–968.
57. Coombs, G. H. and Mottram, J. C. (2001) Trifluoromethionine, a prodrug designed against methionine gamma-lyase-containing pathogens, has efficacy in vitro and in vivo against *Trichomonas vaginalis*. *Antimicrob. Agents. Chemother.* **45**, 1743–1745.
58. Sato, D., Kobayashi, S., Yasui, H., Shibata, N., Toru, T., Yamamoto, M., Tokoro, G., Ali, V., Soga, T., Takeuchi, T., Suematsu, M., and Nozaki, T. Cytotoxic effect of amide derivatives of trifluoromethionine to the enteric protozoan parasite *Entamoeba histolytica*. *Int. J. Antimicrob. Agents*, in press.

59. Colombani, F., Cherest, H., and De Robichon-Szulmajster, H. (1975) Biochemical and regulatory effects of methionine analogs in *Saccharomyces cerevisiae*. *J. Bacteriol.* **122**, 375–384.
60. Duewel, H., Daub, E., Robinson, V., and Honek, J. F. (1997) Incorporation of trifluoromethionine into a phage lysozyme: implications and a new marker for use in protein ^{19}F NMR. *Biochemistry* **36**, 3404–3416.
61. Ito, S., Narise, A., and Shimura, S. (2008) Identification of a methioninase inhibitor, myrsinoic acid B, from *Myrsine seguinii* Lev., and its inhibitory activities. *Biosci. Biotechnol. Biochem.* **72**, 2411–2414.
62. Hirota, M., Miyazaki, S., Minakuchi, T., Takagi, T., and Shibata, H. (2002) Myrsinoic acids B, C and F, anti-inflammatory compounds from *Myrsine seguinii*. *Biosci. Biotechnol. Biochem.* **66**, 655–659.
63. Cellarier, E., Durando, X., Vasson, M. P., Farges, M. C., Demiden, A., Maurizis, J. C., Madelmont, J. C., and Chollet, P. (2003) Methionine dependency and cancer treatment. *Cancer. Treat. Rev.* **29**, 489–499.
64. Kokkinakis, D. M. (2006) Methionine-stress: a pleiotropic approach in enhancing the efficacy of chemotherapy. *Cancer. Lett.* **233**, 195–207.
65. Yoshioka, T., Wada, T., Uchida, N., Maki, H., Yoshida, H., Ide, N., Kasai, H., Hojo, K., Shono, K., Maekawa, R., Yagi, S., Hoffman, R. M., and Sugita, K. (1998) Anticancer efficacy in vivo and in vitro, synergy with 5-fluorouracil, and safety of recombinant methioninase. *Cancer. Res.* **58**, 2583–2587.
66. Tan, Y., Sun, X., Xu, M., Tan, X., Sasson, A., Rashidi, B., Han, Q., Tan, X., Wang, X., An, Z., Sun, F. X., and Hoffman, R. M. (1999) Efficacy of recombinant methioninase in combination with cisplatin on human colon tumors in nude mice. *Clin. Cancer. Res.* **5**, 2157–2163.
67. Kokkinakis, D. M., Hoffman, R. M., Frenkel, E. P., Wick, J. B., Han, Q., Xu, M., Tan, Y., and Schold, S. C. (2001) Synergy between methionine stress and chemotherapy in the treatment of brain tumor xenografts in athymic mice. *Cancer. Res.* **61**, 4017–4023.
68. Hu, J. and Cheung, N. K. (2009) Methionine depletion with recombinant methioninase: in vitro and in vivo efficacy against neuroblastoma and its synergism with chemotherapeutic drugs. *Int. J. Cancer.* **124**, 1700–1706.
69. Miki, K., Xu, M., Gupta, A., Ba, Y., Tan, Y., Al-Refaie, W., Bouvet, M., Makuuchi, M., Moossa, A. R., and Hoffman, R. M. (2001) Methioninase cancer gene therapy with selenomethionine as suicide prodrug substrate. *Cancer. Res.* **61**, 6805–6810.
70. Spallholz, J. E., Palace, V. P., and Reid, T. W. (2004) Methioninase and selenomethionine but not Se-methylselenocysteine generate methylselenol and superoxide in an in vitro chemiluminescent assay: implications for the nutritional carcinostatic activity of selenoamino acids. *Biochem. Pharmacol.* **67**, 547–554.
71. Yang, Z., Wang, J., Yoshioka, T., Li, B., Lu, Q., Li, S., Sun, X., Tan, Y., Yagi, S., Frenkel, E. P., and Hoffman, R. M. (2004) Pharmacokinetics, methionine depletion, and antigenicity of recombinant methioninase in primates. *Clin. Cancer. Res.* **10**, 2131–2138.
72. Sun, X., Yang, Z., Li, S., Tan, Y., Zhang, N., Wang, X., Yagi, S., Yoshioka, T., Takimoto, A., Mitsushima, K., Suginaka, A., Frenkel, E. P., and Hoffman, R. M. (2003) In vivo efficacy of recombinant methioninase is enhanced by the combination of polyethylene glycol conjugation and pyridoxal 5′-phosphate supplementation. *Cancer. Res.* **63**, 8377–8383.
73. Takakura, T., Takimoto, A., Notsu, Y., Yoshida, H., Ito, T., Nagatome, H., Ohno, M., Kobayashi, Y., Yoshioka, T., Inagaki, K., Yagi, S., Hoffman, R. M., and Esaki, N. (2006) Physicochemical and pharmacokinetic characterization of highly potent recombinant L-methionine gamma-lyase conjugated with polyethylene glycol as an antitumor agent. *Cancer. Res.* **66**, 2807–2814.
74. Ravaglia, G., Forti, P., Maioli, F., Martelli, M., Servadei, L., Brunetti, N., Porcellini, E., and Licastro, F. (2005) Homocysteine and folate as risk factors for dementia and Alzheimer disease. *Am. J. Clin. Nutr.* **82**, 636–643.
75. Lonn, E., Yusuf, S., Arnold, M. J., Sheridan, P., Pogue, J., Micks, M., Mcqueen, M. J., Probstfield, J., Fodor, G., Held, C., and Genest, J. (2006) Homocysteine lowering with folic acid and B vitamins in vascular disease. *N. Engl. J. Med.* **354**, 1567–1577.
76. Bønaa, K. H., Njølstad, I., Ueland, P. M., Schirmer, H., Tverdal, A., Steigen, T., Wang, H., Nordrehaug, J. E., Arnesen, E., and Rasmussen, K. (2006) Homocysteine lowering and cardiovascular events after acute myocardial infarction. *N. Engl. J. Med.* **354**, 1578–1588.
77. Ebbing, M., Bleie, Ø., Ueland, P. M., Nordrehaug, J. E., Nilsen, D. W., Vollset, S. E., Refsum, H., Pedersen, E. K., and Nygård, O. (2008) Mortality and cardiovascular events in patients treated with homocysteine-lowering B vitamins after coronary angiography: a randomized controlled trial. *JAMA* **300**, 795–804.
78. Chan, E. C., Chang, P. Y., Wu, T. L., and Wu, J. T. (2005) Enzymatic assay of homocysteine on microtiter plates or a TECAN analyzer using crude lysate containing recombinant methionine gamma-lyase. *Ann. Clin. Lab. Sci.* **35**, 155–160.
79. Han, Q. and Hoffman, R. M. (2008) Enzymatic assay for total plasma Cys. *Nat. Protoc.* **3**, 1778–1781.
80. Han, Q., Xu, M., Tang, L., Tan, X., Tan, X., Tan, Y., and Hoffman, R. M. (2002) Homogeneous, nonradioactive, enzymatic assay for plasma pyridoxal 5-phosphate. *Clin. Chem.* **48**, 1560–1564.
81. Manukhov, I. V., Mamaeva, D. V., Rastorguev, S. M., Faleev, N. G., Morozova, E. A., Demidkina, T. V., and Zavilgelsky, G. B. (2005) A gene encoding L-methionine gamma-lyase is present in enterobacteriaceae family genomes: identification and characterization of *Citrobacter freundii* L-methionine gamma-lyase. *J. Bacteriol.* **187**, 3889–3893.
82. Land, K. M., Delgadillo-Correa, M. G., Tachezy, J., Vanacova, S., Hsieh, C. L., Sutak, R., and Johnson, P. J. (2004) Targeted gene replacement of a ferredoxin gene in *Trichomonas vaginalis* does not lead to metronidazole resistance. *Mol. Microbiol.* **51**, 115–122.
83. Mirelman, D., Anbar, M., and Bracha, R. (2008) Trophozoites of *Entamoeba histolytica* epigenetically silenced in several genes are virulence-attenuated. *Parasite* **15**, 266–274.

Mitosomes in *Entamoeba histolytica* contain a sulfate activation pathway

Fumika Mi-ichi, Mohammad Abu Yousuf, Kumiko Nakada-Tsukui, and Tomoyoshi Nozaki[1]

Department of Parasitology, National Institute of Infectious Diseases, Tokyo 162-8640, Japan

Edited by Andrew Roger, Dalhousie University, Halifax, NS, Canada, and accepted by the Editorial Board October 19, 2009 (received for review June 25, 2009)

Hydrogenosomes and mitosomes are mitochondrion-related organelles in anaerobic/microaerophilic eukaryotes with highly reduced and divergent functions. The full diversity of their content and function, however, has not been fully determined. To understand the central role of mitosomes in *Entamoeba histolytica*, a parasitic protozoon that causes amoebic dysentery and liver abscesses, we examined the proteomic profile of purified mitosomes. Using 2 discontinuous Percoll gradient centrifugation and MS analysis, we identified 95 putative mitosomal proteins. Immunofluorescence assay showed that 3 proteins involved in sulfate activation, ATP sulfurylase, APS kinase, and inorganic pyrophosphatase, as well as sodium/sulfate symporter, involved in sulfate uptake, were compartmentalized to mitosomes. We have also provided biochemical evidence that activated sulfate derivatives, adenosine-5′-phosphosulfate and 3′-phosphoadenosine-5′-phosphosulfate, were produced in mitosomes. Phylogenetic analysis showed that the aforementioned proteins and chaperones have distinct origins, suggesting the mosaic character of mitosomes in *E. histolytica* consisting of proteins derived from α-proteobacterial, δ-proteobacterial, and ancestral eukaryotic origins. These results suggest that sulfate activation is the major function of mitosomes in *E. histolytica* and that *E. histolytica* mitosomes represent a unique mitochondrion-related organelle with remarkable diversity.

anaerobic protozoa | evolution | mitochondria | organelle | proteomics

Diversification of mitochondrial structure and function has occurred during eukaryotic evolution, and was especially observed in anaerobic/microaerophilic environments. Most extant anaerobic eukaryotes, which were previously considered to lack mitochondria, are now regarded to possess reduced and highly divergent forms of mitochondrion-related organelles (1, 2). The hydrogenosome is an organelle in which hydrogen and ATP are produced, and is found in anaerobic protists and fungi such as *Trichomonas vaginalis* (3, 4), *Neocallimastix patriciarum* (5, 6), and *Nyctotherus ovalis* (7). The mitosome, typically demonstrated in parasitic and free-living protists such as *E. histolytica* (2, 8–15), *Giardia intestinalis* (16, 17), diverse microsporidian species (18–20), and *Cryptosporidium parvum* (21), generally has reduced functions and does not produce hydrogen or ATP. In *Mastigamoeba balamuthi*, a mitochondrion-related organelle was discovered and presumed to possess a unique array of biochemical properties, although it remains unclear whether the organelle is more similar to either hydrogenosomes or mitosomes (22). In contrast, the mitochondrion-related organelle in *Blastocystis* contains DNA and shows characteristics for both hydrogenosomes and mitochondria of higher eukaryotes (23). Organisms that possess hydrogenosomes and mitosomes do not cluster together in eukaryote phylogenies, indicating that secondary losses and changes in mitochondrial functions have independently occurred multiple times in eukaryote evolution (1). Although hydrogenosomes and mitosomes are divergent in their contents and functions, a number of shared characteristics have been previously suggested, which include a double membrane, mitochondrial chaperonin 60 (Cpn60), and the iron sulfur cluster (ISC) system (1). However, recent studies indicate that *E. histolytica* and *M. balamuthi* lack the ISC system, and instead possess the nitrogen fixation (NIF) system, which is most likely derived from an ancestral nitrogen fixing ε-proteobacterium by lateral gene transfer (22, 24). Only 5 proteins have been demonstrated in *E. histolytica* mitosomes: Cpn60 (8–10, 12), Cpn10 (13), mitochondrial Hsp70 (11, 15), pyridine nucleotide transhydrogenase (PNT) (2, 8), and mitochondria carrier family (MCF, ADP/ATP transporter) (14), and the central role of mitosomes in *E. histolytica* remains unknown. Analysis of the genome of *E. histolytica* has not revealed any additional information regarding the function of mitosomes and thus, a proteomic analysis of mitosomes seems to be the best approach to understand its structure and function (1, 2).

In this study, we examined the proteomic profile of purified mitosomes and showed by immunofluorescence assay that a repertoire of proteins were localized to mitosomes, and demonstrated by enzymological studies that some of these mitosomal proteins were associated with sulfate activation. We further showed by phylogenetic analysis that mitosomes are a mosaic organelle consisting of components derived from at least 3 distinct origins. This study identifies that sulfate activation is the major function of mitosomes in *E. histolytica*.

Results

Identification of Mitosomal Proteins. To elucidate the central role of mitosomes in *E. histolytica*, we took a proteomic approach to identify the proteins associated with mitosomes. We developed an improved purification scheme, consisting of 2 consecutive discontinuous Percoll gradient centrifugations that yielded an enriched mitosomal fraction suitable for proteome analysis [supporting information (SI) Fig. S1]. The presence of mitosomes was monitored with the authentic mitosomal marker Cpn60. Mitosomes were recovered from fractions 19 and 20 in the first centrifugation and from fractions I through K in the second centrifugation with a peak in fraction J (Fig. 1). A list of mitosomal proteins was made by subtracting the proteins identified in fractions G and O from those in fraction J, as fraction J contained traces of either lysosome or ER protein, which were detected by markers cysteine protease 5 (CP5) and Sec61α, respectively (Fig. 1).

Survey of the Mitosomal Proteome. Three independent mitosomal purifications and MS analysis reproducibly identified 95 putative mitosomal proteins (Table S1). Although 64 of the proteins identified were annotated in the *E. histolytica* genome database as "hypothetical protein," 3 enzymes involved in sulfate activation—ATP sulfurylase (AS) (25), APS kinase (APSK), and inorganic pyrophosphatase (IPP)—were identified as dominant constituents, based on the high coverage obtained for each protein (as described

Author contributions: F.M. and T.N. designed research; F.M., M.A.Y., and K.N.-T. performed research; F.M. contributed new reagents/analytic tools; F.M. and T.N. analyzed data; and F.M. and T.N. wrote the paper.

The authors declare no conflict of interest.

This article is a PNAS Direct Submission. A.R. is a guest editor invited by the Editorial Board.

[1]To whom correspondence should be addressed. E-mail: nozaki@nih.go.jp.

This article contains supporting information online at www.pnas.org/cgi/content/full/0907106106/DCSupplemental.